SYNTHESIS AND CHARACTERIZATIONS OF ZINC OXIDE NANOPARTICLES FOR ANTIMICROBIAL APPLICATIONS

A Thesis Submitted to Applied Physics Program Adama Science and Technology University

For Partial Fulfillment of the Requirements for the Degree of Master of Science in Physics

By: MideksaKasahun

Advisor: Abebe Belay (Associate Professor)

Jully, 2018

Adama, Ethiopia

APPROVAL SHEET

ADAMA SCIENCE AND TECHNOLOGY UNIVERSITY

SCHOOL OF APPLIED NATURAL SCIENCE

APPLIED PHYSICS PROGRAM

This is certifying that the thesis prepared by Mideksa Kasahun entitle **"Synthesis and Characterization of zinc oxidenanoparticles for antimicrobial applications"** submitted in fulfillment of the requirement for the degreeof master of science in physics complies with the regulation of the university and meets the accepted standards with respect to originality.

Signed by the examination committee

and meets the accepted standards with respect to originality.

Signed by the examination committee

Name Signature Date

....

(Advisor)

....

(Co-Advisor)

....

(Chairman)

....

(External Examiner)

....

(Internal Examiner)

ACKNOWLEDGEMENT

First of all, I am gratefully indebted to the almighty God whose everlasting and undying love kept me and for his infinite mercy throughout my life and during the course of this thesis work.

My sincere gratitude thanks go to my advisor Dr. Abebe Belay for his patience; understanding, Financial support and critical concerns made this research work a great success.

I acknowledge and appreciate my beloved classmates and friends all those who contributed in one way or the other to the fulfilment of this research work specially AlayehuNugusawho are closest as two faces of one-coinfriendship to me.

I would like to acknowledge Pusan National University, Department of Nanofusion Technology, South Korea for allowing, UV-Vis, Photoluminescence, SEM characterization of my sample. My immeasurable thanks further go toLemmaTeshome who have worked the characterization of my sample.

I would like to acknowledge the advanced physics and biology laboratory of ASTU for allowing me to use essential materials of this research work.

I have no words to express my gratitude thanks to Mr.Urgessa who have assisted me the microbial laboratory activity Micro biology laboratory of ASTU.

I would like to express my gratefulness thanks to Dr. Mesfin Asfaw, head department of physics, for his willingness and support me by writing a letter towards other institutions, and to Dr. Tewodros Yirgashewa, Dr. MegersaWedajo and Dr. Alemu Kebede too for feed me immeasurable knowledge in the corresponding courses.

Finally, my immeasurable thanks go to my wonderful and caring parents specially, my wife SenaKaba, my father KasahunFufaand my mami, my Brother Garomakasahunfor their love, moral, and financial support towards my research.

Dedication

This work is dedicated to:

My Wife SenaKaba

My father: KasahunFufa

My mother: KibituWirtu

My littlest brother: GaromaKasahun

Contents

1. Introduction **1**

2. Literature review **2**

2.1. Zinc oxide nanoparticles *2*

2.2. Crystal structures of ZnO *3*

2.3. Electronic properties *4*

2.4. Chemical properties of ZnO *5*

2.4.1. Optoelectronic properties of ZnO *5*

2.5. Methods of synthesis *6*

2.6. Characterization techniques of ZnO nanoparticles *7*

2.7.1. X-ray diffraction (XRD) 7

2.7.2 Scanning Electron Microscopy (SEM) 10

2.7.3. UV-Visible Spectroscopy 11

2.7.4. Fourier Transform Infrared (FT-IR) Spectroscopy 13

2.7.5. FluorescenceSpectroscopy 15

2.7. Antimicrobial applications of zinc oxide nanoparticles *17*

3. Materials and Methods **22**

3.1. Chemicals and solvents *22*

3.3. Synthesis methods *23*

3.3.1. Synthesis of S-1 and S-2ZnO NPs 23

3.3.2. Synthesis of S-3ZnO NPs 23

3.3.3. Synthesis of S-4, S-5 and S-6ZnO NPs 23

3.4. Methods of characterization *24*

3.4.1. XRD characterization 24

3.4.2. SEM characterization 24

3.4.3. UV- Vis spectroscopy characterization 25

3.4.4 Fluorescence spectroscopy characterization 25

3.4.5. FT-IR spectroscopy characterization 25

3.5. Antimicrobial activity procedures *26*

4. Results and Discussions **27**

4.1 X-Ray Diffraction Analysis *27*

4.2. SEM Analysis *34*

4.3. UV-Vis absorption Analysis *36*

4.8. Emission Spectra analysis *37*

4.4. Antimicrobial activity of the ZnO nanoparticles *39*

5 Conclusions and Recommendations **44**

5.1 Conclusions *44*

References **45**

List of figures

Figure Page

Fig 2.1. a). Hexagonal wurtzite structure of ZnO b). Cubic zinc blende structure of ZnO c). Unit cell of ZnO 4

Fig 2.2: a schematic of various optical process of absorption, excitation and subsequent radiative recombination among discrete energy state of Zno NPs. 17

Fig. 2.3. Correlation between the influence of essential ZnO NPs parameter on the antibacterial Response and the different possible mechanisms of ZnO NPs antibacterial activity, including ROS formation, Zn^{2+} release Internalization of ZnO NPs in to bacteria and electrostatic interactions..... 21

Fig4.1a The XRD spectra of S-1 and S-2 ZnO NPs 27

Fig4.1b. The XRD spectra of S-3 ZnO NP. 28

Fig 4.1c The XRD spectra of S-4, S-5 and S-6 ZnO NPs..... 28

Fig 4.2a, b. The XRD powder diffraction spectra of (101) oriented peaks show increase in intensity as temperature increase for S-1, S-2, b. for S-4, S-5, and S-6. 31

Fig. 4.3a, b. W – H plot for synthesized ZnO NPs S-1 and S-2. 31

Fig.4.4. The relation between crystallite size and energy band gap. 32

Fig. 4.5 The colorations b/n crystallite size and Dislocation density 33

Figure 4.5: Flower shape of Scanning Electron Microscope images for S-2 ZnO NPs. 35

Fig.4.6. Thesperical shape of Scanning Electron Microscope image of S-4 ZnO NPs 36

Fig 4.7: Absorption spectra of S-1, S-3, S-4, S-5 and S-6 ZnO NPs. 37

Fig. 4.8. The emission spectra of S-1 and S-6 ZnO NPs 38

Fig4. Thebar graphs showing zone of inhibition introduced by S-1, S-3, S-4, S-5 ZnO NPs at 3.14mM, 6.34mM, 12.63mM and Gentamicinagainst S. aureus 41

Fig 4.10a, b thebar graphs showing zone of inhibition introduced by S-1, S-3, S-4, S-5 ZnO NPs and Gentamicinagainst E. coli, P. aeruginosa, S. aureus, B. subtills, S. typhi and C. albicans 42

Fig4.11a, b shows inhibition zone of S-3 ZnO NPs on E.coli and S-1 ZnO NPs on S. aureus 43

List of Abbreviations

B. subtilis	*Bacillus subtilis*
C. albicans	candida albicans
E. coli	Escherichia coli
FT-IR	Fourier Transform Infrared
FWHM	Full width at half- maximum
GRAS	Generally recognized as safe
MIC	Minimum Inhibitory concentration
P. aeruginosa	*Pseudomonas aeruginosa*
ROS	Reactive oxygen species
S. aureus	Staphylococcus aureus
SEM	Scanning electron microscopy
UV/Vis	Ultraviolet visible
XRD	X-ray diffraction
ZnO NPs	Zinc oxide nanoparticles
ZnO	Zinc oxide
ZOI	Zone of inhibition

Abstract

In this study, the ZnO nanoparticles were synthesised from precursors $Zn(NO3)_2.6H_2O$ and $Zn(CH3COO)_2.2H_2O$ by using Sol- gel, thermal decomposition and Precipitation method respectively. The synthesized ZnO NPs characterized using X-Ray Diffraction (XRD), Fourier Transform Infrared (FTIR), UV-Vis spectroscopy, Scanning Electron Microscopy (SEM) and Fluorescence Spectroscopy. From XRD results the synthesized ZnO NPs have wurtzite hexagonal structure and its crystallite sizes increase as the temperature increases, the lattice parameters (a and c) are temperature dependent i.e. an increase in temperature leads to expansion of lattice parameters due to this the volume of cell decreasing and spacing between the lattice planes decreasing when annealing temperature increase. The morphology of ZnO NPs was characterized by SEM. It indicated that S-2 and S-4 ZnO NPs was flower and spherical shape and the particle size of S-4 greater than S-1 ZnO NPs which agree with XRD result. The optical absorption of ZnO NPs measured at different annealing temperatures indicates red shift as the temperature increases. The ZnO NPs were showed two emission bands, an ultraviolet emission band due to the transition from conduction band edge to valence band, and visible emission band due to defects that are related to deep level emissions. The synthesised ZnO NPs were applied for antimicrobial activity on Gram-negative bacteria E. coliand P. aeruginosa, Gram-positive bacteria S. aureus B. subtilis and S. typhi and Fungus candida albicans using well diffusion agar method. All synthesisedZnO NPs were showed admirable antibacterial activity. Among synthesisedZnO NPs, the S-3 ZnO NP which was synthesized using thermal decomposition method was showed excellent antibacterial activity.

Key words: ZnO NPs, sol-gel method, thermal decomposition method, precipitation method, spectroscopic techniques and antimicrobials.

1. Introduction

Nanoscience is a branch of science which deals about nanomaterials that displays significant properties that are not available in bulk materials and exhibit vast applications due to their small size [1].Nanoparticles are the class of materials and remarkable scientific tools that has been used for various biotechnological, pharmacological and technological uses. They are cornerstones of nanoscience and nanotechnology. Nanoparticles are different from bulk materials due to their small size, higher surface area to volume ratio, crystallographic surface structure, specific magnetic properties and new quantum effects. They also exhibit unique physical and chemical properties which exist due to the presence of a high concentration of defects like electrical, catalytic, magnetic, mechanical, thermal, or imaging features [3]

Nanoparticles are grouped into organic and inorganic nanoparticles; however inorganic nanoparticles are more applicable due to their ability to withstand harsh processing conditions present in many industries. Nanomaterials may be metals, ceramics, polymers as well as composites. Metal elements have better performance to form a large diversity of oxide compounds used in the fabrication of microelectronic circuits, sensors, piezoelectric devices, fuel cells, coatings for the passivation of surfaces against corrosion [4].

Metal oxide nanoparticles have distinctive interest to researchers because of their multifunctional properties. They display novel and enhanced physical, chemical and biological properties due to their nanoscale dimensions, low melting point, high mechanical strength, high density of corner and random motion. They also show emerging optical, magnetic, electrical and catalytic properties [5].Among various inorganic metal oxide

nanoparticles, ZnO nanoparticles have their own importance due to their vast area of applications. It has tremendous scientific and technological interest [6].

Zinc oxide is an extrinsic n-type ultrafine semiconductor material with a chemical formula ZnO [7]. It is a direct-band gap material in which the maximum energy of the valence band and the minimum of the conduction band occur at the same value of the momentum. Oxygen has the highest ionization energy, which leads to a strongest interaction between the Zn3*d*- and O2*p*-orbitals [8]. Due to this strong interaction, ZnO is having a direct wide band gap energy (3.37ev), high exciton binding energy (60mev), high electron mobility [9], higher breakdown field strength, higher quantum efficiency, noncentral symmetry and excellent chemical stability. It is nontoxic and naturally occurs as the rare mineral zincite. But, ZnO which used for commercial purposes is produced synthetically. It is transparent to visible range of spectrum and exhibits unique optical, electric conductivity and piezoelectric properties [10].It also has high electrochemical coupling coefficient, broad range of radiation absorption, biocompatibility, biodegradability and high photostability property [11].

Nowadays, zinc oxide is an interesting topic to researchers due to its significantly unique and essential morphology such as Nano rods, Nano flowers, nanowires, nanodendriter and nanoparticles [12, 13]

ZnO is the most significant compound for electronic and optoelectronic applications such as solar cells (anti-reflecting coating and transparent conducting materials), varistors, luminescence, electrostatic dissipative coatings, transparent UV protection films, gas sensors, liquid crystal displays, heat mirrors, surface acoustic wave devices etc due to its high optical transparency and luminescent properties in the near ultraviolet and the visible regions [14]

It has a great potential in sunscreens, ointments, creams and lotions due to its ability to reflect the skin deteriorating UV radiation.ZnO NPs powder is widely used as an additive intonumerous materials and products including plastics, ceramics, glass, adhesive, ferrites,sealants, cement, rubber manufacturing, lubricants, batteries, fire retardants, etc. It has beenused in food industry for food supplements, breakfast cereals and animal feedstuffs as a source of zinc nutrient [16].

Currently, Zinc oxide nanoparticles have vast applications in various industrial areas due to their exceptional characteristics such as anti-corrosion, ultraviolet filtering, catalytic, low electrons conductivity and excellent heat resistance. They are used in paints, solar cells as window layers' electronics, stain-resistant clothing, UV light-emitting devices, photocatalysis, electronics, water filtrations and pharmaceuticals products.They are also used in textile and cosmetics industries due to their higher surface area to volume ratio, high UV absorption and pyroelectric properties. Due to their significant optical, electrical, and magnetic properties.ZnO nanoparticles have crucial role in communications, sensing, data storage, optics, transmission, environmental protection, biology, and medicine. They are also used in sunscreens as an ultraviolet- resistant additive and in a range of textile.

Zinc oxide nanoparticles have vast biomedical application without coating because of their non-central symmetry, bio safe, less toxicity, antibacterial activity, effective drug delivery, tumor targeting, anti- inflammatory activity, bio absorption and biocompatibility, imaging features and piezoelectric properties [3]. They show a higher degree for selections of cancer cell with the ability exceed the therapeutic indices of a few universally used chemotherapeutic agents.

They also play a very important role in cellular adhesion and uptake due to their high fluorescence and electrostatic nature. ZnO NPs have also great application for antimicrobial activity in food packaging and processing industries because of reactive oxygen species that induced on their surface [16]

Many researchers have been synthesised and characterized zinc oxide nanoparticles, and studied antibacterial activities depend on size, concentration, dimensions and morphology of nanoparticles [17]. The antimicrobial activity of zinc oxide nanoparticles have been studied against Gram-negative bacteria*Escherichia coli* and Gram-positive *Staphylococcus aureus.* They have been reported that Gram-positive bacteria have higher susceptibility to zinc oxide nanoparticles than Gram-negative bacteria due to their polarity difference of cell membrane, structural difference in bacterial membrane and the difference in intracellular antioxidant content [18].

On the other hand, as far as our knowledge concerns there is no research reports on comparison study of ZnO NPsusing sol–gel, precipitation and thermal decomposition methods and study their antimicrobials activity like against Gram-positive (*S. aureus*, Salmonella Typhi *Bacillus subtilis)*, Gram-negative (*Pseudomonas aeruginosa* and *E. coli*) bacterial strains andfungus (Candida Albicans)

Therefore, the General objective of this study was synthesis ZnO NPs using Sol-gel, thermal decomposition and precipitation methods and characterize it using spectroscopic techniques for antimicrobial applications.

The specific objectives of this study were: 1. SynthesisZnONPs using sol-gel method from precursor$Zn(NO3)_2.6H_2O$ and polymer PVA at different annealing temperatures. 2.

Synthesis ZnONPs using thermal decomposition method from precursor $Zn(CH3COO)_2.2H_2O$.3.SynthesisZnONPs using precipitation method from $Zn(CH3COO)_2.2H_2O$andprecipitating agent NaOHat different annealing temperatures. 4. Characterize the synthesizedZnONPs using spectroscopic techniques such as XRD,SEM, UV-Vis Spectroscopy, FT-IR Spectroscopy and Fluorescence Spectroscopy. 5. Determining antimicrobial activity of synthesized ZnO NPs using well diffusion methods for different pathogenic bacteria and fungus.

The thesis is organized as follows: In chapter 1, introduction to nanoscience and nanoparticles, metal oxide NPs and zinc oxide, general synthesis routes of ZnO nanoparticles, the applications of ZnO NPs and objectives of the study are presented.

In chapter 2, literature reviews related to ZnO NPs are presented. The ZnO NPs, the crystal structures, chemical, Electrical and optoelectronic properties of ZnO and the synthesis methods of ZnO NPs are discussed. Furthermore, the characterizations techniques (XRD, SEM, UV-Vis Spectroscopy, Fluorescence Spectroscopy and FTIR Spectroscopy) of ZnONPsand application of ZnO NPs for antimicrobial activities

In chapter 3, the materials and methods of the study are presented. This chapter has six sections; in the first and the second sections of this chapter, the various chemicals, solvents and apparatus used to carry out this research work are described respectively. In the third, fourth and fifth sections, the methods of synthesis and characterization are presented respectively. In section six, the antimicrobial activity procedures are presented.

In chapter 4, the results and discussions of the thesis are presented. The average

crystallite size, micro strain, dislocation density, lattice parameters, volume of cell was calculated and UV-Vis absorption peak, emission spectra and FT-IR spectra of ZnO NPs are reported. In the final section of this chapter, antimicrobial activities of ZnO NPs are reported. Finally, the conclusion of the thesis is drawn in chapter 5.

2. Literature review

2.1. Zinc oxide nanoparticles

Among various inorganic semiconductor metal oxide nanoparticles, ZnO nanoparticles are the most functional, strategic, promising, and versatile material due to their high surface area to volume ratio, low toxicity, high chemical stability and biocompatibility [19]. They have neutral hydroxyl groups attached to their surface, which play a key role in their surface charge behavior [20].

The physical and chemical properties of zinc oxide nanoparticles depend on their composition, size and shape. Optical property is one the most fundamental and functional aspects of ZnO NPs. It is depending on some parameters such as size, shape, surface characteristics, doping and interaction with the surrounding environment or other nanostructures. Due to their optical properties ZnO NPs are applicable in optical detector, laser, sensor, imaging, photocatalysis, photoelectrochemistry and biomedicine.

The optical property of ZnO nanoparticles is mainly measured by different spectroscopic techniques. ZnO NPs have been used for targeted imaging of cancer cells, sensing, fighting human pathogens, healthcare products and photodynamic therapy due to their nontoxicity because of their magnetic properties. They have a great potential for biological application due to their quantum effects which can affect the chemical reactivity and other physical and chemical properties, and the similarity of nanoparticles and biomolecules in dimension.

The ZnO nanoparticles have useful applications in textile industry since ZnO coating is more air permeable and efficient UV-blockers compared with any other semiconductor material

[21]. ZnO NPs have more toxic effects on bacteria and fungi due to some factors like light intensity, surface chemistry and particle morphology. However, they have minimal effect onhuman cells[3].

2.2. Crystal structures of ZnO

Zinc oxide has three crystal structures such as hexagonal wurtzite, cubic zinc blende and cubic rocksalt. Among these, wurtzite crystalline structure is the most stable phase at ambient conditions. In this structure every zinc atom is tetrahedrally coordinated with four oxygenatoms. It has lattice parameters, a = 0.32495 nm and c = 0.52069 nm, ratio of c / a =1.6023,which is similar to the ideal value of hexagonal cell *c/a* = 1.633. It belongs to the space group of $P6_3mc$ and is characterized by two interconnecting sublattices of Zn^{2+} andO^{2-}. The cubic rocksalt is observed only at relatively high pressures ~10 GPa. The tetrahedral symmetry of wurtzite structure makes an imperative role for the polarity of ZnO that arises along the hexagonal axis. The polar symmetry of ZnO along the hexagonal axis results piezoelectricity, pyroelectricity and spontaneous polarization. Since ZnO has sensitive lattice constants to the presence of structural point defects (oxygen vacancies and interstitial Zn ions act as donors in its lattice) and extended defects (threading/planar dislocations), it has an n-type nature. These structural point and extended defects are commonly found in ZnO resulting in a non-stoichiometric compound $Zn_{1+d}O$ with excess zinc. They are responsible for visible photoluminescence [9, 10, 11]. Fig 2.1 shows crystal structures of ZnO.

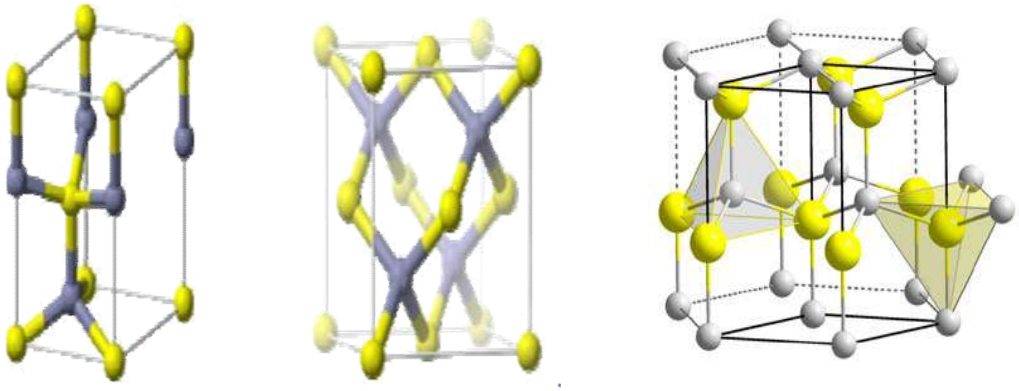

a b c

Fig 2.1. a). Hexagonal wurtzite structure of ZnOb). Cubic zinc blende structure of ZnO c). Unit cell of ZnO

2.3. Electronic properties

ZnO has a relatively large direct band gap of 3.37 eV at room temperature. One of the advantages associated with a large band gap include higher breakdown voltages, ability to sustain large electric fields, lower electronic noise and high- temperature and high-power operation. Most ZnO has *n*-type character, even in the absence of intentional doping. Native defects such as oxygen vacancies or zinc interstitials are often assumed to be the origin of this, but the subject remains controversial. An alternative explanation has been proposed, based on theoretical calculations, that unintentional substitutional hydrogen impurities are responsible.

Controllable n-type doping is easily achieved by substituting Zn with group-III elements Al, Ga, In or by substituting oxygen with group-VII elements chlorine or iodine. Reliable p-type doping of ZnO remains difficult. This problem originates from low solubility of p-type

dopants and their compensation by abundant n-type impurities, and it is pertinent not only to ZnO, but also to similar compounds GaN and ZnSe. Measurement of p-type in "intrinsically" n-type material is also not easy because inhomogeneity results in spurious signals [21].

2.4. Chemical properties of ZnO

Pure ZnO is occurs as a white powder usually called as white zincite or mineral zincite. Because crystalline ZnO is thermo-chromic, its color is changing from white to yellow when it is heated in air. It also reverts to white on cooling due to a very small loss of oxygen at high temperature to form the non-stoichiometric $Zn_{1+x}O$. Since zinc oxide is an amphotericoxide, it is insoluble in water and alcohol, but in most acids like hydrochloric acid and in alkalis.

ZnO forms cement like material which are used in dentistry when reacted with phosphoric acid and a strong aqueous solution of zinc chloride. It produces carboxylates like asoleate or stearate when react with fatty acids in oils [10, 11]

2.4.1. Optoelectronic properties of ZnO

The optical properties of ZnO are heavily influenced by the energy band structure and lattice dynamics. The processes of optical absorption and emission have been influenced by an extrinsic transition called bound exciton. This bound exciton is related to defects which are responsible for creating discrete electronic states in the band gap. Exciton can be bound with neutral or charged donors and acceptors and it depends on the band structure of semiconductor material. Thus, bound exciton does not require traps to localize carriers and recombines with high efficiency.

Zinc oxide films which made from single crystal can be applied for modulation of UV radiation due to its directionally dependent optical property. It is also used for different electronic application due to its high breakdown stress and high saturation velocity. Due to its higher radiation, chemical, and thermal resistance, ZnO is used to form transparent contacts of solar cells. Fluorescence spectra of ZnO nanowire shows increase of green emission intensity with a decrease of nanowire diameter and continuous reduction of diameter of ZnO nanowire gives quantum size effect and due to this size confinement exciton binding energy is enhanced. The performance of optoelectronic devices have been influenced by transport characteristics and interaction of phonon with free carrier [22].

2.5. Methods of synthesis

Currently there are number of physical and chemical method of synthesizing ZnO NPs such as chemical vapor deposition[48], sol–gel[31], spray pyrolysis[48], co-precipitation method[30], and thermal decomposition method [38], etc. However, in above synthesis methods a strictly controlled synthesis environment, high synthesis costs, complexities in synthesis reaction, expensive equipment and complicated operation should be considered. So, it is still a need for a simple method to synthesize ZnO NPs with mass-scale yield production. Among various methods, thermal decomposition is one of the most common methods for synthesis of ZnO nanoparticles. In present work, a simple, low-cost, catalyst free and direct mass-scale production method is applied for the preparation of high-purity ZnO nanoparticles.

2.6. Characterization techniques of ZnO nanoparticles

In order to apply ZnO NPs for any of applications characterization should be hold after synthesis of the material. Several physical techniques have been developed to characterize the size, morphology, crystalline structure, temperature effects and other remarkable properties of ZnO NPs. The most commonly used characterization techniques are X-ray diffraction (XRD), Scanning Electron Microscopy (SEM), UV-Visible Spectroscopy, Fluorescence Spectroscopy and FT-IR Spectroscopy. The detail information about these techniques is explained as follows.

2.7.1. X-ray diffraction (XRD)

X-ray is an energetic electromagnetic radiation appearing at the region between gamma-rays and ultraviolet, which is comparable with the size of an atom. When X-rays interact with a crystalline substance (phase), one gets a diffraction pattern. The reflection of incident monochromatic X-ray from successive planes of crystal lattices when the difference between the planes of complete number n of wavelengths leads to famous Bragg's law [22]. TheBragg's law can be described according to equation (2.1).

$$nd = 2\lambda \sin\theta \qquad (2.1)$$

Where n is an integer 1, 2, 3..., λ is wavelength in nanometer, d is interatomic spacing and θ is the diffraction angle in degree.

XRD can used to characterize nanoparticles such as ZnO NPs. It determines the average crystallite size, Micro strain, Dislocation density, bond length between Zn and O Atoms and etcof ZnO NPs. A great advantage of X-ray powder diffraction is that it requires

virtually no sample preparation, in comparison to other characterization techniques.

The sample can be either in the form of smear or compact flat pack or a capillary and is exposed to monochromatic beam of x-ray and the diffracted beam intensity is collected in a range of angles (2θ) with respect to the incident beam. The intensity corresponding to a constructive interference of the diffracted beam from a crystallographic plane is observed as peak, corresponding to the Bragg angle (θ). A powder diffraction pattern contains information on phases present (peak positions), phase concentrations (peak heights), structure, degree of crystallinity or amorphous content (background hump) and crystallite size/strain.

The width of the peaks in a particular phase pattern provides an indication of the average crystallite size. Large crystallites give rise to sharp peaks, while the peak width increases as crystallite size decreases. Crystallite size does not equal the size of the particle, as one particle can be a conglomerate of several crystallites.

Peak broadening also occurs as a result of variation in d-spacing caused by micro strain. The positions of the peaks provide an accurate fingerprint of the crystal structure of the nanocrystals. The average crystallite size of the ZnONPs can be obtained from the line broadening using Debye Scherer formula [23, 24] according to equation (2.2).

$$D = \frac{0.9\lambda}{\beta \cos\theta} \tag{2.2}$$

For a hexagonal system like ZnO, lattice constants $a = b \neq c$ and crystallographic axes $\alpha = \beta = 90^{\circ}$, $\gamma = 120^{\circ}$. In our case, the lattice constant a is calculated only for those XRD peaks for

which $l = 0$ (i.e. *hk0* peaks) and lattice constant c is calculated only for those XRD peaks for which $h = k = 0$ (i.e. *00l* peaks). Applying these conditions in eq. (3), we obtain the following equations, respectively for the calculation of a and c.[25]

$$a = \frac{\lambda}{\sqrt{3}\sin\theta}\sqrt{h^2 + hk + k^2} \tag{2.3}$$

$$c = \frac{\lambda}{2\sin\theta} l \tag{2.4}$$

$$\frac{1}{d^2} = \frac{4}{3}\left\{\frac{h^2 + hk + k^2}{a^2}\right\} + \frac{l^2}{c^2} \tag{2.5}$$

$$V = 0.866 a^2 c \tag{2.6}$$

The strain induced broadening in powders due to crystal imperfection and distortion was calculated using the formula[21].

$$\mu_s = \frac{\beta}{4\tan\theta} \tag{2.7}$$

the total peak broadening is represented by the sum of the contributions of crystallite size and strain present in the material and can be written as [22],

$$\beta = \frac{0.9\lambda}{D\cos\theta} + \mu_s \sin\theta \tag{2.8}$$

The dislocation density, which represents the amount of defects in the sample is defined as the length of dislocation lines per unit volume of the crystal and is calculated using the Eq. [24],

$$\delta = \frac{1}{D^2} \tag{2.9}$$

Where D is the crystallite size andis dislocation density

The Zn-O bond length L is given by [24,25]

$$L = \sqrt{(\frac{a^2}{3} + (\frac{1}{2} - u)^2 c^2)} \tag{2.10}$$

Where u is the positional parameters in the wurtzite structure and is a measure of the amount by which each atom is displaced with respect to along the 'c' axis. 'u' is given by

$$u = \frac{a^2}{3c^2} + 0.25 \tag{2.11}$$

The correlation between the c/a ratio and u is that when the c/a ratio decreases, the u increases in such a way that those four tetrahedral distances remain nearly constant through a distortion of tetrahedral angles

2.7.2 Scanning Electron Microscopy (SEM)

Scanning electron microscopy (SEM) is a microscopic instrument which gives detail information about size, external morphology (texture), microstructure ofZnO nanoparticles. Electrons are thermionically emitted from a tungsten or lanthanum hexa boride cathode and are accelerated towards an anode; alternatively, electrons can be emitted via field emission. The electron beam, which has an energy ranging from a few hundred eV to 100 KeV, is focused by one or two condenser lenses in to a beam. Characteristic X-rays are emitted when the primary beam causes the ejection of inner shell electrons from the sample and are used to

determine the elemental composition of the sample.

As most biological specimens are made up of non-dense material the amount of secondary electrons produced is too low to be of much use in creating an image and therefore they are usually coated with a very fine layer of a metal which readily produces secondary electrons. The back scattered electrons emitted from the sample can be used.Thesesignals are monitored by photomultiplier tubes and magnified. An image of the investigated microscopic region of the specimen is observed in cathode ray tube and is photographed [25].

2.7.3. UV-Visible Spectroscopy

UV-visible Spectroscopy is the type of absorption spectrophotometer which involves the excitation of electrons present in the molecule from ground state to excited state. It is the most reliable and accurate analytical method which used to measure scanning or transition of electron and optical properties of materials. Absorption spectrophotometer is the analytical technique in which compounds absorb light of radiation of a specific wavelength.spectrophotometer is an instrument used to measure the transmittance and absorbance of a sample as a function of the wavelength of electromagnetic radiation. Absorbance (A) is the amount of light that is absorbed by a sample, while transmittance (T) is the amount of light transmitted through a sample.

UV-Vis spectroscopy is almost entirely used for quantitative analysis in which the estimation of the amount of a compound known to be present in the sample solution. The components of UV-Vis spectroscopy are light source that generates a broad band of electromagnetic radiation, monochromater (wavelength selector), sample holder, detector to measure the intensity of radiation and computer (read signal). The absorption spectra of

atoms, molecules, or ions are generated when a beam of electromagnetic energy or light is passed through a sample, and absorbs a portion of the photons of electromagnetic energy passing through the sample [27].

UV-Vis spectroscopy can alsousedto characterize the nanoparticles such ZnO nanoparticles. It measures the absorption peak of ZnO nanoparticles, which occurred due totransition or scanning of electron from valence band to conduction band.

When an electron gets some amount of photon energy from UV or visible light, it is jumping from valence band (lower energy) to conduction band (higher energy).It is the peculiar property for ZnO. The absorption peak is depending on some factors like selection of wavelength, nature of the solvent, band gap, oxygen deficiency, size and structure of the nanoparticles, surface roughness, impurity centres, PH of the solution and temperature.

Generally, as it was reported in several literatures, the UV-Vis absorption peaks of ZnO NPs are found between 350 nm- 380 nm[27, 28].The width of energy gap of ZnO NPs calculated based on effective mass approximation using Brus Equation [31].

$$E_{g_{(nano)}} = E_{g(bulk)} + \frac{h^2}{8R^2}\left(\frac{1}{\mu_e} + \frac{1}{\mu_h}\right) - \frac{1.8e^2}{4\pi\varepsilon_0\varepsilon_r R^2} \qquad (2.12)$$

Where, $E_{g(nano)}$, $E_{g(balk)}$ are the width of band energy gap (eV) for nanomaterials and bulk semiconductor ZnO. The other parameters such as h represents Plank constant, R is particles radius, μ_e and μ_h are electron and hole effective mass, e, $e, \varepsilon_r, \varepsilon_0$ are the charge of the electron, dielectric constant and electric permittivity of free space respectively.

h = Planck constant =4.125x10^{-15} eV

m_e =effective mass of excited electron =$2.14x10^{-31}$

m_h= effective mass of excited hole =$5.37x10^{-31}$

hR= radius of quantum dot =D/2=R=calculated from EQ.1

e = electronic charge $1.602x10^{-19}$

permittivity of vacuum =$8.85x10^{-12}$

Relative permittivity =8.66

E_{bulk}=3.37eV

2.7.4. Fourier Transform Infrared (FT-IR) Spectroscopy

FTIR Spectroscopy is a non-destructive and highly flexible instrument which able to measure bond vibrational motions of atoms in molecules. It is a powerful technique for chemical characterization, identification of functional groups and used to achieve information regarding the attachment of the capping agents. In recent time, it has been replaced dispersive instruments for most applications due to its superior speed and sensitivity [32].

The three basic spectrometer components of FTIR spectroscopy are radiation source, interferometer and detector. It uses a beam of infrared light to analyze the structure of organic compounds, identify unknown materials, and determine the quality or consistency of a sample and the amount of components in a mixture [33]. FTIR analyze a wide range of materials in bulk or thin films, liquids, solids, pastes, powders, fibers, and other forms. Its

spectra of pure compounds are generally so unique that they are like a molecular "fingerprint" [34].

Vibrational motion of atoms in a molecule is influenced by the masses of atoms, their geometrical arrangement and strength of their chemical bonds. There are IR and Raman spectra, which are the results of transition between quantized vibrational states and provide a complementary image of molecular vibrations. Both IR and Raman spectra involves IR radiation [33].

Specific types of chemical bonds or functional groups can be identified by infrared spectroscopy based on their unique absorption signatures. Identification of functional groups is the cornerstone of IR spectroscopy, which produces broad absorptions. Molecules absorb resonant frequencies that are characteristic of their structure. This means the frequency of the absorbed radiation matches the frequency of the bond or group that vibrates and the detection of energy is done on the basis of shape of the molecular potential energy surfaces, the masses of the atoms, and the associated vibronic coupling. IR encompasses a spectral region from red end of visible spectrum (12500 cm^{-1}) to 10 cm^{-1}regions in the electromagnetic spectrum

It is the most influential tool to identify compounds by matching spectrum of unknown compound with reference spectrum (finger printing) and functional groups in unknown substances. IR is commonly divided into near IR (12500 to 4000 cm^{-1}), mid IR (4000 to 400 cm^{-1}) and far IR (400 to 10 cm^{-1}). Among these, mid IR(4000 to 400 cm-1) spectra region is the most significance and richest region in chemical information due to the occurrence of the most fundamental molecular vibrations [33, 34].

FT-IR spectroscopy also used to characterize ZnO NPs to investigate their vibrational motions. It gives detail information about the surface chemistry of ZnO nanoparticles and functional groups attached to the zinc oxide nanoparticles surface. These functional group shows various FT-IR pattern than those of free groups. Zinc oxide generally gives vibrational phonon in fingerprint region from 400 cm^{-1}- 600 cm^{-1} arising from inter-atomic vibrations. The IR spectra of ZnO NPs greater than 600 cm^{-1} is due to some other carboxylic and hydroxyl groups like O-H, C=O, C-H, C-O, which are attached to zinc oxide nanoparticles during synthesis [34].

2.7.5. FluorescenceSpectroscopy

Fluorescence Spectroscopyis a rapid, sensitive and selective characterization method. It is a contactless and non-destructive method to investigate the electronic structure of materials. It is also a type of electromagnetic spectroscopy that analyzes fluorescence from a sample using a beam of ultraviolet light. This beam of light excites the electrons in molecules of certain compounds and causes them to emit light. In the single molecule fluorescence spectroscopy, intensity fluctuations from the emitted light are measured from either single fluorophores or pairs of fluorophores [33].

Fluorescence spectroscopy measures the intensity of photons emitted from a sample, an excitation spectrum and emission spectrum. The three basic parts of fluorescence spectroscopy are source of light, sample holder and detector. Photons impinge on the excitation monochromator, which selectively transmits lightin a narrow range centered about the specified excitation wavelength.

The transmitted light passes through adjustable slits that control magnitude and resolution by further limiting the range of transmitted light. The filtered light passes into the sample cell causing fluorescent emission by fluorophores within the sample. Emitted light enters the emission monochromater, which is positioned at a 90º angle from the excitation light path to eliminate background signal and minimize noise due to stray light. Again, emitted light is transmitted in a narrow range centered about the specified emission wavelength and exits through adjustable slits. Spectral resolution and signal to noise is directly related to the selected slit widths. The particle cannot emit energy at the place where it was absorbed [33, 34].

Fluorescence spectroscopy also used to characterize nanoparticles such ZnO NPs. This technique involves measuring the energy distribution of emitted photons after optical excitation of ZnO nanoparticles. Since ZnO is a semiconductor, free electrons are there in the conduction band and holes are in the valence band. When electrons make a transition from ground state to excited state because of some photon energy which is emitted from the source, energy is absorbed. While this electron came back to valence band, emission is occurred i.e energy is emitted. The emission spectra of ZnO nanoparticles have been exceed their absorption spectra due to their semiconducting properties. This is implies when some amount of radiation (photon) is supply, electrons are climb from valence band (lower energy) to conduction band (higher energy), and when it came backs to valence band (lower energy) from conduction band (higher energy), the wavelength is greater since photon energy is inversely proportional to wavelength. Generally, ZnO exhibits two kinds of emissions: one is at ultraviolet near band-edge emission and the other a visible deep level emission with a peakin the range from 450 to 700 nm. The UV emission is related to the transition from

conduction band edge to valence band. The Visible emission spectra is caused by the transition from deep donor level to valence band due to oxygen vacancies and by the transition from conduction band to deep acceptor level due to impurities and defectstates[34].

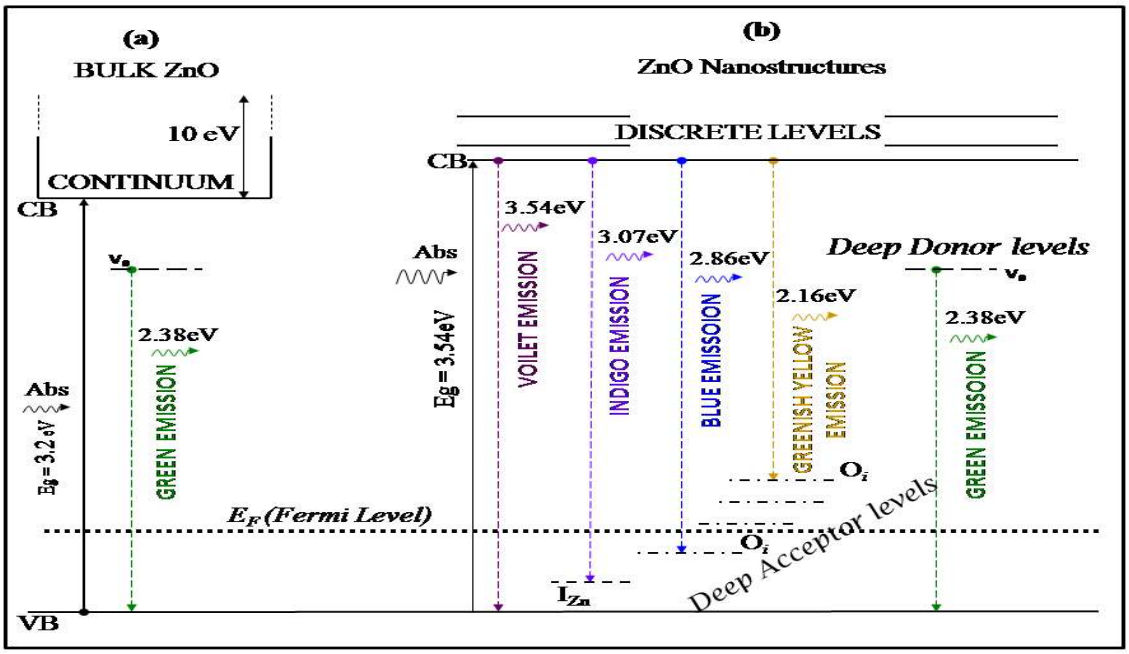

Fig 2.2: a schematic of various optical process of absorption, excitation and subsequent radiative recombination among discrete energy state of Zno NPs.

2.7. Antimicrobial applications of zinc oxide nanoparticles

Now a days, Zinc oxide is listed as a generally recognized as safe (GRAS) material by the Food and Drug Administration and it is used as food additive. Zinc is an essential micronutrient which used for intensification, improvement and health in humans and animals [16].The three mechanisms for the antimicrobial activity of ZnO nanoparticles are the release of antimicrobial ions, interaction of nanoparticles with microorganisms [36] and the formation of ROS [17].

The antimicrobial influence of ZnO NPs can be due morphologies, UV illumination effect, Size and concentration, surface modification by thermal annealing, surface charge and defects. Many studies have reported that the toxicity is significantly affected by the various morphologies of ZnONPs [38,39]. In this regard, the shape of ZnO NPs can influence their mechanism of internalization such as rods and wires penetrating into cell walls of bacteria more easily than spherical ZnO-NPs [38]. Whereas, flower-shaped have revealed higher biocidal activity against S. aureus, and E. coli than the spherical and rod-shaped ZnO NPs [38].

Particle size and concentration of ZnONPs play important roles in the antimicrobial activity. Larger surface area and higher concentration are accountable for ZnONPs in the antimicrobial activity [40]. ZnONPs of smaller sizes can easily penetrate into bacterial membranes due to their large interfacial area, thus enhancing their antibacterial efficiency A large number of studies investigated on the considerable impact of particle size on the antibacterial activity, and the researchers found that controlling ZnONPs size was crucial to achieve best microbial response, and ZnONPs with smaller size (higher specific surface areas) showed highest antibacterial activity [40]

ZnO NPs possess high photocatalytic efficiency among all inorganic photocatalytic materials, and is more biocompatible than TiO_2 [40]. ZnO can highly absorb UV light [41], and it has a better response to UV light, thus its conductivity dramatically enhances, and this feature significantly activates the interaction of ZnO with bacteria. Its photoconductivity persists long after turning off the UV light, and it cause surface electron depletion region strongly associated to negative oxygen species (O_2^{-2}, O_2^-) adsorbed on the surface [41].UVillumination rapidly causes desorption of this loosely bound oxygen from the

surface. This results in reducing the surface electron depletion region and causing improved photoconductivity [42]. The photocatalysis is described as a photo-induced oxidation process that can damage and in-activate organisms [43]. ZnO-NPs in aqueous solution under UV radiation have phototoxic effect that can produce ROS such as hydrogen peroxide (H_2O_2) and superoxide ions (O^{2-}). Such species are extremely essential for bio-applications [42].Thegenerated active species are capable to penetrate into the cells, thus inhibit or kill microorganisms. This process inspired the use of the photocatalytic activity of ZnO-NPs in bio nanotechnology and in bio-nanomedicine for many antimicrobial applications.

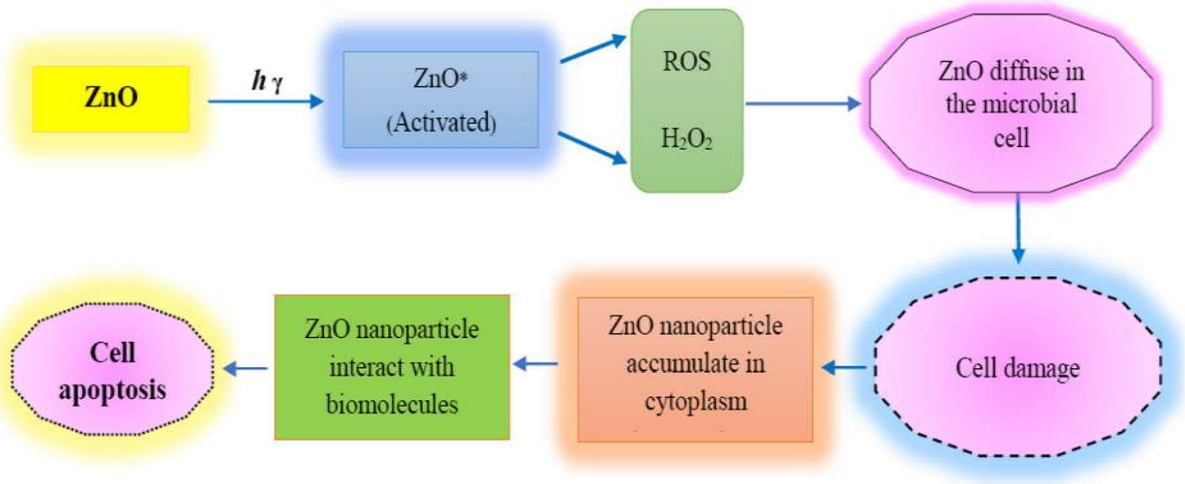

Fig.2.3. The UV illumination of ZnO NPs cause the cell apoptosis of microbials

The electronic band structure of ZnO, as a semiconductor material consists of a conduction band (CB) and a valence band (VB). Incident radiation with photons of energy greater than 3.3 eV is immediately absorbed, thus the electrons move from the VB to the CB. This electron transfer initiates a series of possible photoreactions. As a result, positive holes (h+) are formed in the VB, while free electrons are created within the CB [43].This positive hole (h+), a direct oxidant and essential for the creation of reactive hydroxyl radicals (OH•),serves as principal oxidants in the photocatalytic system [38-40].The electrons in the CB reduce

oxygen, which is adsorbed by the photo-catalyst [22]The proposed an association between photon reaction and the antibacterial activity in a series of reactions resulting in production of hydrogen peroxide (H_2O_2) molecules which penetrates the membrane, causing fatal damage.

Oxygen annealing stimulated a high amount of oxygen atoms to be absorbed onto ZnO surface, thereby enhanced antibacterial response inducing more ROS in the suspension resulting in intense oxidative stress towards the bacteria. and it has shown a considerable increase of O:Zn ratio of the oxygen annealed samples. Modifying ZnONPs surface area would establish the release of Zn^{2+} ions and enhance ROS production. [41] incident radiation with photon energy of ZnO compared to its band gap energy (~3.37eV). As a result a positive area, an electron hole (h+) in the valence band and a free electron (e−) in the conduction band is formed [42].

The electron hole (h+) reacts with H_2O molecules (from the suspension of ZnO) separating them into •OH and H^+; and O_2 molecules dissolved in the medium are transformed into superoxide anion radicals (O_2^-), which in turn react with H^+ and generate (HO_2•). Consequently, this species collides with electrons producing hydrogen peroxide anions (HO_2). Thus, the hydrogen peroxide anion reacts with hydrogen ions to produce H_2O_2 molecules [37].

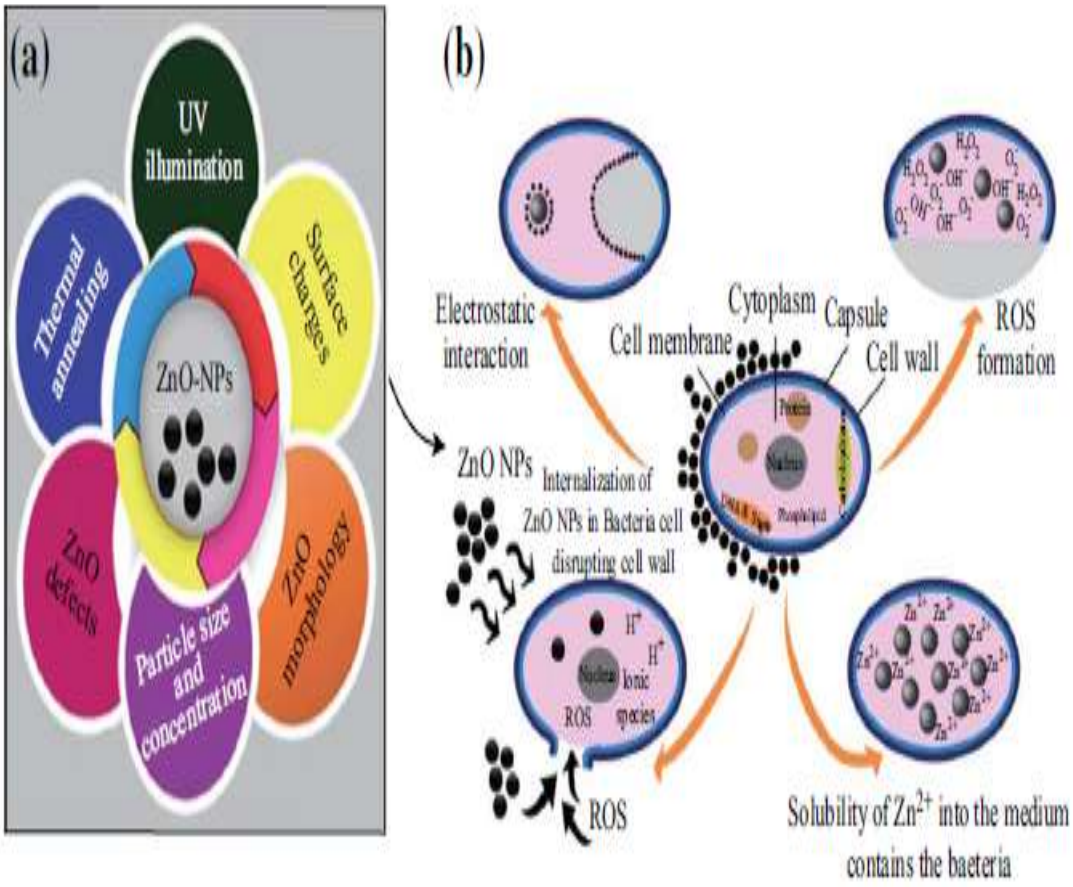

Fig. 2.4. Correlation between the influence of essential ZnO NPs parameter on the antibacterial Response and the different possible mechanisms of ZnO NPs

3. Materials and Methods

3.1. Chemicals and solvents

The chemicals used for the synthesisof zinc oxide nanoparticles and antimicrobial application are zinc nitrate hexahydrate ($Zn(NO3)_2.6H_2O$), (Himedia, India), Polyvinyl Alcohol (PVA) (Himedia, India)sodium hydroxide(NaOH) (Alpha chemika, India), zinc acetate dihydrate($Zn(CH3COO)_2.2H_2O$), (Uni-Chem, India),Mueller Hilton agar (MHA) (M173-500G) (Hi media India), Tryptone soya Agar (Cm 0131) Japan, Nutrient broth (NB) (M173-500G) (Hi media India) And the solvents like deionized water, DMSO(Uni-Chem, India) were used. All the chemicals are analytical grade and do not undergo further purification.

3.2. Apparatus

The apparatus used for synthesis and characterize ZnO NPs are magnetic stirrer with hot plate(MH 21t) India, Whatman filter paper(3001845) England, glass rod, spatula, analytical balance (FA2104) China with accuracy 0.0001g, different sizes of beakers and sample holders, crucible, puddle, Heating oven (DHG-9055) china , Box – type resistance furnace (BK-5-12GJ) china, Bacteriological Incubator ( ) china, Electric Heated vertical steam sterilizer (LX-B751) china, petri dishes, cotton swab, stain less steel cork borer, and 1cm quartz cuvette.

3.3. Synthesis methods

3.3.1. Synthesis of S-1 and S-2ZnO NPs

The S-1 and S-2 ZnO NPs were synthesized by sol-gel method. A 6 gm of Polyvinyl Alcohol were dissolved in 60 ml of double distilled water and stirred by magnetic stirrer for 30 min. Again a 2 gm of zinc nitrate hexa-hydrate ($Zn(NO_3)_2.6H_2O$) also dissolved in 20 ml of double distilled water and stirred by magnetic stirrer for 15 min. Following zinc nitrate hexa-hydrate ($Zn(NO_3)_2.6H_2O$) solution was added into Polyvinyl Alcohol (PVA) solution drop by drop near about 70 ^{0}C under suitable magnetic stirring for 2 hrs. The mixture solution should be stirred till the gel like substances formed; this gel type sample was allowed to dry in oven at 160□ for 12 hrs. The sample was annealed in furnace for 8 hrs at the temperature of 400□. By similar procedures, the other samples (S-2) were prepared at annealing temperatures of 500□

3.3.2. Synthesis of S-3ZnO NPs

The S-3 ZnO NPs was synthesized According to the procedures developed by [46]. A15 gm ofthe zinc acetate dihydrate Zn $(CH_3COO)_2 2H_2O$ was used as the precursor to synthesize ZnO NPs. It was placed into a crucible and calcined at 400^{0}C for 3hour reaction times in furnace without any special atmospheric condition and ZnO NPs are obtained in powder form.

3.3.3. Synthesis of S-4, S-5 and S-6ZnO NPs

The S-4, S-5 and S-6 ZnO NPs was synthesized according to the procedures developed by

[45]. A 12 gm of Zn $(CH3COO)_2.2H_2O$ was dissolved in 100 ml of deionized water in a beaker and stirred for 30 minutes using magnetic starrier at the temperature of 60 ^{0}c. Similarly, 3 gm of NaOH was dissolved in 40 mlof deionized water in a separate beaker and stirred for 15 minutes. The solution of sodium hydroxide was added to the beaker containing Zn $(CH3COO)_2.2H_2O$ solution with constant stirring. The aqueous solution turned into a milky white colloid without any precipitation. The reactionwas allowed to proceed for 2 hours after complete addition of sodium hydroxide. Then, the solution was allowed to settle and filter using Whatman filter paper. The filtered sample was allowed to dry in oven at 160 ^{0}c for 4 hours, and calcined for 2 hours at temperature of 200 ^{0}C, 300 ^{0}C, 500 ^{0}C for S-4, S-5, S-6 respectively infurnace.

3.4. Methods of characterization

3.4.1. XRD characterization

The X-ray diffraction (XRD) pattern for ZnO nanoparticles were analyzed using XPERT-PRO X-ray diffractometer by generating Cu-K_α radiation (λ=1.5418Å). It is used to determine the crystalline phase of the synthesized nanoparticles. An X-ray generator operates at a voltage of 40kV and applied current of 30mA at room temperature. Intensities were measured at room temperature for angle range of $2\theta = 10^0 \leq 2\theta \leq 100$.

3.4.2. SEM characterization

The morphological feature of synthesized ZnO NPs were determined by using Scanning Electron Microscopy (SEM) (Hitachi, H-7600), using electron beam energy of 10 KV and 15

KV. The synthesized ZnO NP powder is mounted on a sample holder followed by coating with a conductive metal. Then, the sample was scanned with focused fine beam of electrons. The surface characteristics of the sample were obtained from the secondary electrons emitted from the sample surface.

3.4.3. UV- Vis spectroscopy characterization

The UV-Vis absorption peaks of ZnO NPs were recorded with UV-Vis spectroscopy (Perkin-ElmerLambda 19 UV-Vis Spectrophotometry with double monochromator using 1 cm fused quartz cuvette) in the wavelength region of 260 - 600 nm at room temperature. The ZnO NPs were dissolved in DMSO and its absorbance measured using 1cm quartz cuvette. The ASC files of the measured spectra were collected by computer which interfaced with the instrument. Finally, the absorption spectra of ZnO NPs were analyzed using origin 8 software.

3.4.4 Fluorescence spectroscopy characterization

The emission spectra of ZnO NPs were measured with fluorescence spectroscopy (FLS1000 photoluminescence spectrometer) having Single-Cell accessory type, excitation width slit of 10 nm in the wavelength region of 350-700 nm at room temperature and excitation wave length of 325 nm. The samples were dissolved in DMSO and stirred until it dissolved. The emission spectra of the sample were measured by 1 cm quartz cuvette.

3.4.5. FT-IR spectroscopy characterization

The vibrational phonon and the quality of ZnO NPs were also characterized by Fourier transform infrared spectroscopy( ) in the wavenumber region of 4000-400 cm^{-1} according to

the procedures reported by [31]. The ZnO NPs spectra measurements were performed by putting the powder ZnO NPs on KBr pellet.

3.5. Antimicrobial activity procedures

The antimicrobial activity of the synthesizedZnO NPs on microbialswere tested by Well diffusion agar method according to the procedures reported by [43]. One loop of each bacteria and Fungus were sub-cultured aerobically in 10ml nutrient broth for 24 hours at 37^0C in incubator.A 2mM(162.76µg/ml)stoke solution of S-1, S-3, S-4 and S-5 ZnO NPs was prepared in DMSO and stirred using magnetic terrier for 30 minutes at room temperature, using Dilution equation from 0.1- 2mM concentration of each sample was prepared to check antimicrobial activity or to determine MIC of synthesized ZnO NPs. A 0.01ml of sub-cultured bacteria were spread using sterilized cotton swab on about 30ml of sterilized molten and cooled MHA media for pathogenic bacteria and TSA for fungus were poured in sterilized, washed and dry petri dishes. 8mm well prepared using sterilized stainless steel corkborerand properly labeled. About0.1mlof each ZnO NPs solution having different concentration was poured on each six well on all petri dishes using micropipe.and waiting Until it properly diffuse and ready to inoculate. Control experiments were also carried out in the presence of known impregnated standard antibiotic drugs vancomycin. After inoculation the diameters of the inhibition zones were measured in millimeters after 24hour incubation times.

4. Results and Discussions

4.1 X-Ray Diffraction Analysis

Figure 4.1a-c shows the XRD pattern of ZnO nanoparticles synthesised using Sol-gel, Thermal decomposition Precipitation method at different annealing temperature respectively. All the diffraction peaks of the synthesized ZnO NPs correspond to (100), (002), (101), (102), (110), (103), (200), (112) and (201) of crystal planesare almost matched with standard ZnO powder (ICDD No. 80-0074). No diffraction peaks from other species could be observed which indicates that all the precursor have been completely decomposed and no other crystal products have been retained after the decomposition process. The (101) crystal plane peak is the most intense peaks that shows plane is preferred growth plane.The sharp peaks indicate that the products are well crystallized.

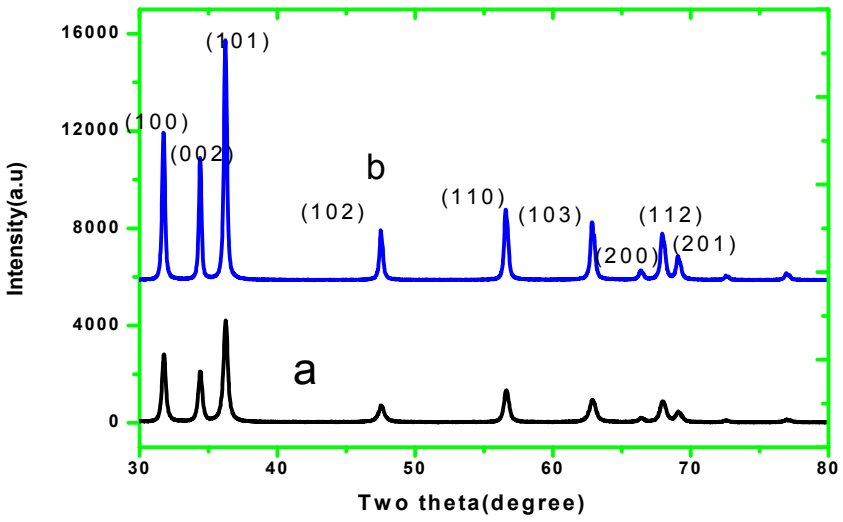

Fig4.1a The XRD spectra of S-1 and S-2 ZnO NPs

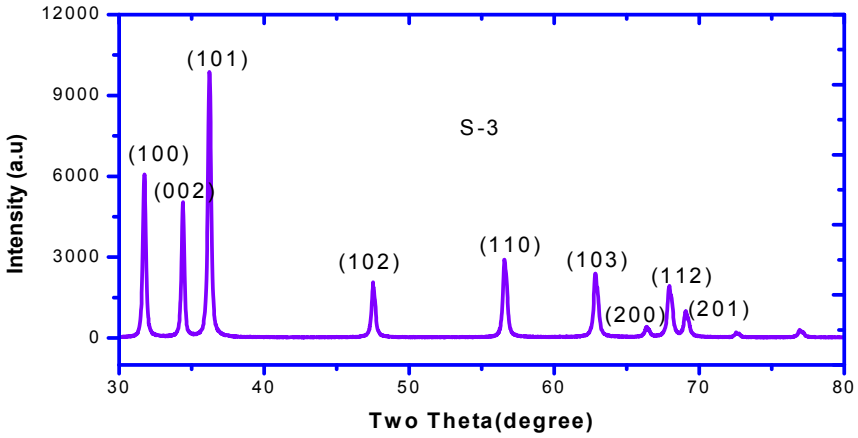

Fig4.1b. The XRD spectra of S-3 ZnO NP.

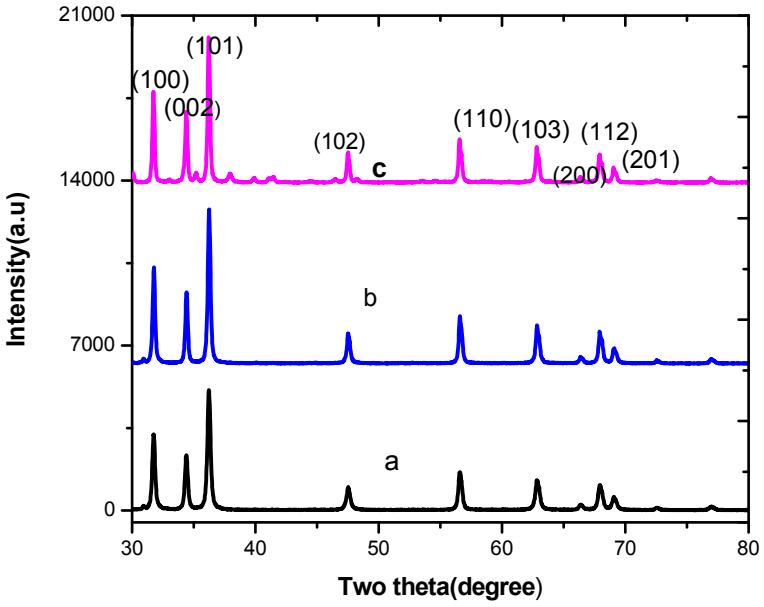

Fig 4.1c The XRDspectra of S-4, S-5 and S-6ZnO NPs

The average crystallite size of the ZnO NPs calculated using Debye Scherer formula [23, 24]. According to this equation (2.2) it is from table 4.1: 22.04 ± 2 nm, 29.38 ± 2 nm, 29.92 ± 1 nm, 29.30 ± 4 nm, 36.90 ± 3 nm, 41.67 ± 2 nm for S-1, S-2, S-3, S-4, S-5 and S-6 synthesized ZnO NPs respectively.

For the synthesized ZnO NPs the lattice parameters a, c, interplanar distance (d_{hkl}) and volume of the cellwas calculated and tabulated in table4.2.using [25] eq(2.3), (2.4), (2.5) and (2.6).The standard ZnO powder is crystallized in a hexagonal system with lattice parameter a=3.2535, c=5.2151 and space group is P63mc (186).Therefore, the lattice parameters (*a* and*c*) calculated for prepared nanoparticles are in good agreement with the published crystallographic data for ZnO and the lattice parameters are temperature dependent i.e. an increase in temperature leads to expansion of lattice parameters which clearly observed on table 4.2.From Braggs law eq(2.1) and table 4.2spacing between the lattice planes decreasing when annealing temperature increase. This is reasonable for a small particle, where a large part of the atoms is located close to the surface where there can be some relaxation in the bonding as the surface atoms have fewer neighbors to bind to than the corresponding bulk atoms.The unit cell volume for the synthesizedZnO NPs was $47.513(nm)^3$, $47.71(nm)^3$, $47.713(nm)^3$, $47.642(nm)^3$, $47.578(nm)^3$and $45.410(nm)^3$ for S-1, S-2, S-3, S-4, S-5 and S-6 respectively this shows when temperature increase the volume of cell decrease due elongation of lattice parameters.

Figure 4.2a, b. shows the diffraction peak intensity markedly increases with annealing temperature and due to high annealing temperature provides sufficient energy to crystallites and to orient in proper equilibrium sites and causes an increase in intensity [17-18].

At higher annealing temperature peaks become more and more intense with reduced broadening, which indicate the increase in grain size with increasing temperature [13].

Table 4.1: The synthesized ZnONPs and its crystallite size

Name of synthesized ZnO NPs	Average crystallite size (nm)
S-1ZnO NPs	22.04 ± 2
S-2ZnO NPs	29.38 ± 2
S-3ZnO NPs	29.30 ± 4
S-4ZnO NPs	29.92 ± 1
S-5ZnO NPs	36.90 ± 3
S-6ZnO NPs	41.67 ± 2

Table 4.2: The lattice parameter a, c, c/a, volume of the cell and interplanar spacing of synthesized ZnO NPs calculated from XRD results.

Synthesized ZnO NPs	lattice parameter			$V(nm)^3$	$d_{(101)}$(nm)
	a(nm)	c(nm)	c/a		
S - 1	0.3246	0.52072	1.6041897	47.513	0.247749074
S - 2	0.3252	0.520963	1.6019772	47.711	0.24774905
S - 3	0.3252	0.520981	1.6020325	47.713	0.247746451
S - 4	0.32501	0.520812	1.6024491	47.642	0.247628754
S- 5	0.3249719	0.520561	1.6023577	47.578	0.247507575
S- 6	0.3252688	0.495621	1.5237274	45.410	0.244908146

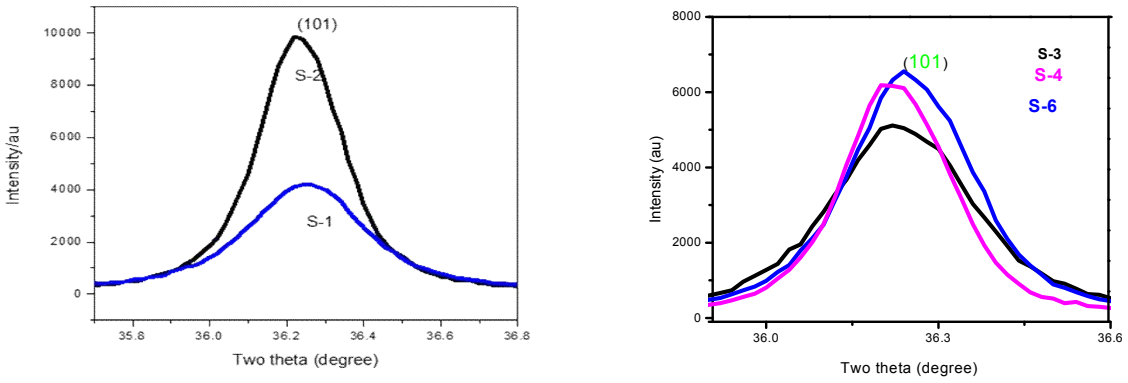

a b

Fig 4.2a, b. The XRD powder diffraction spectra of (101) oriented peaks show increase in intensity as temperature increase for S-1, S-2, b. for S-4, S-5, and S-6.

Fig4.3a, b Shows the Williamson–Hall (W–H) plot analysis of lattice strain which affect the Bragg peak in different ways and both these effects increase the peak width, peak intensity and shift the diffraction angle peak position accordingly.

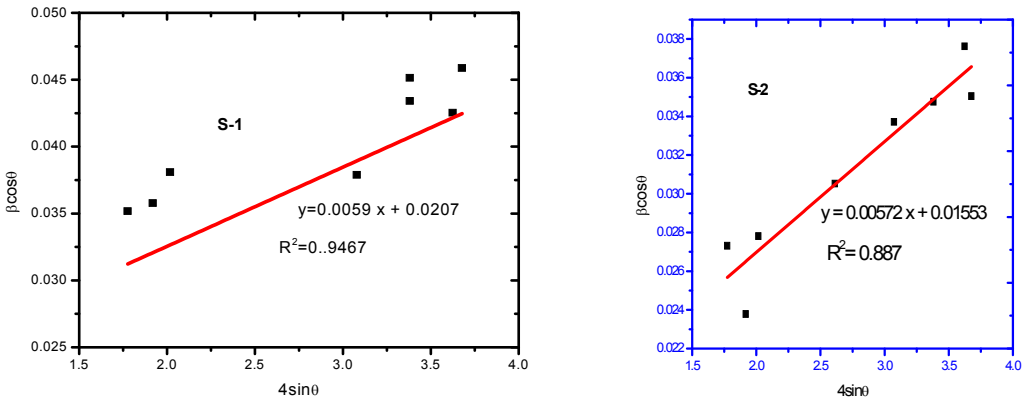

a b

Fig. 4.3a,b. W – H plot for synthesized S-1and S-2ZnO NPs.

According to [31] eq (2.12) the energy gap of synthesized ZnONPs was 3.48 eV, 3.43eV, 3.43 eV, 3.43 eV, 3.41eV and 3.40 eV forS-1, S-3, S-4, S-5 and S-6 respectively. And Figure.4.3. and Table 4.3 shows the increasing in crystallite size cause decrease in energy band gap of ZnONPs.

Table4.3: Crystallite size of synthesizedZnO NPs and its energy band bap.

Crystallite size(nm)	E_g(eV)
22.04	3.484456
29.38	3.434410
29.31	3.434718
29.92	3..432106
35.65	3.4137464
41.67	3.4020195

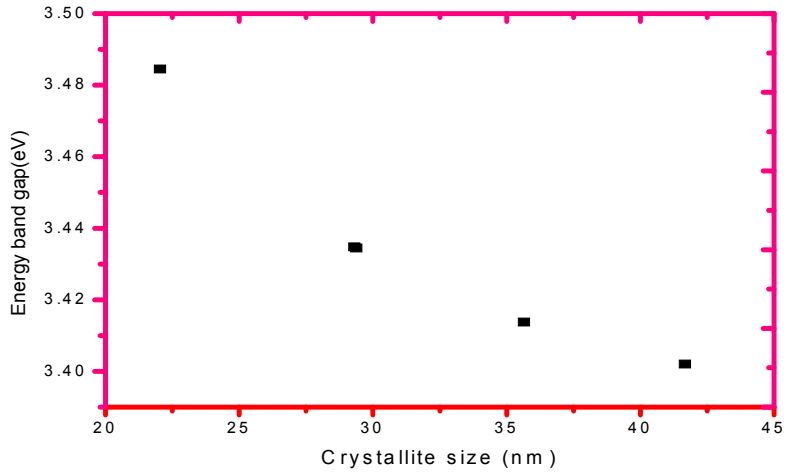

Fig.4.4. The relation between crystallite size of Zno NPs and its energy band gap.

The dislocation density (δ), which represents the amount of defects in the sample is defined as the length of dislocation lines per unit volume of the crystal and is calculatedusing the Eq (2.9) [24] becomes the following. Where D is crystallite size the dislocation density of eachwas

$20.58\times10^{-4}(nm)^{-2}$,$11.58\times10^{-4}(nm)^{-2}$,$11.64\times10^{-4}(nm)^{-2}$,$11.17\times10^{-4}(nm)^{-2}$,$7.34\times10^{-4}(nm)^{-2}$a nd $5.75\times10^{-4}(nm)^{-2}$ respectively. As shown in Fig.4.5. Dislocation densities exhibits a decreasing trend with increasing temperature.

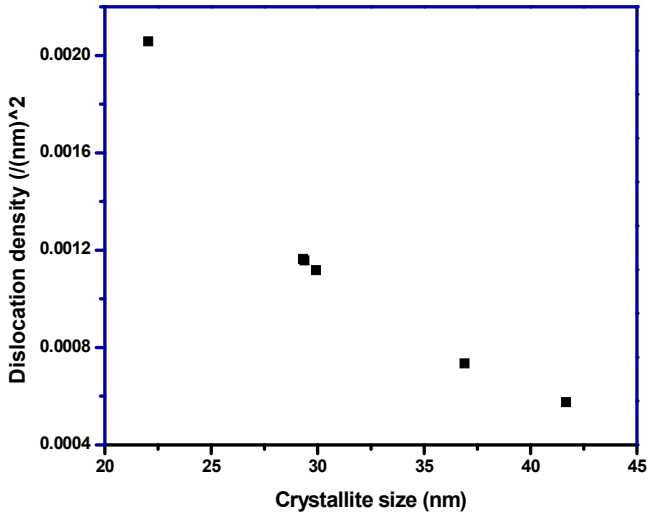

Fig. 4.5 The colorations b/n crystallite size of ZnO NPsand its dislocation density

The Zn-O bond length L is given by eq (2.12) [26].Where u is the positional parameters in the wurtzite structure and is a measure of the amount by which each atom is displaced with respect to the along the ‘c’ axis. ‘u’ is given by eq (2.13) [26].The correlation between the c/a ratio and u

is that when the c/a ratio decreases, the u increases in such a way that those four tetrahedral distances remain nearly constant through a distortion of tetrahedral angles. The Zn–O bond length calculated is 0.19762nm, 0.19790nm, 0.197895nm, 0.1978099nm, 0.197722nm, and 0.195061nm respectively. Wereas the reported Zn–O bond length in the unit cell of ZnO and neighboring atomsis 0.19767 nm [29]. The calculated bond length agrees with the Zn–O bond length in the unit cell.

4.2. SEM Analysis

Figure4.5a, b shows the SEM images S-2 and S-4 ZnO NPs. As it shown the morphology of the S-2 ZnO NPs was flower shape and S-4 ZnO NPs was spherical shape.

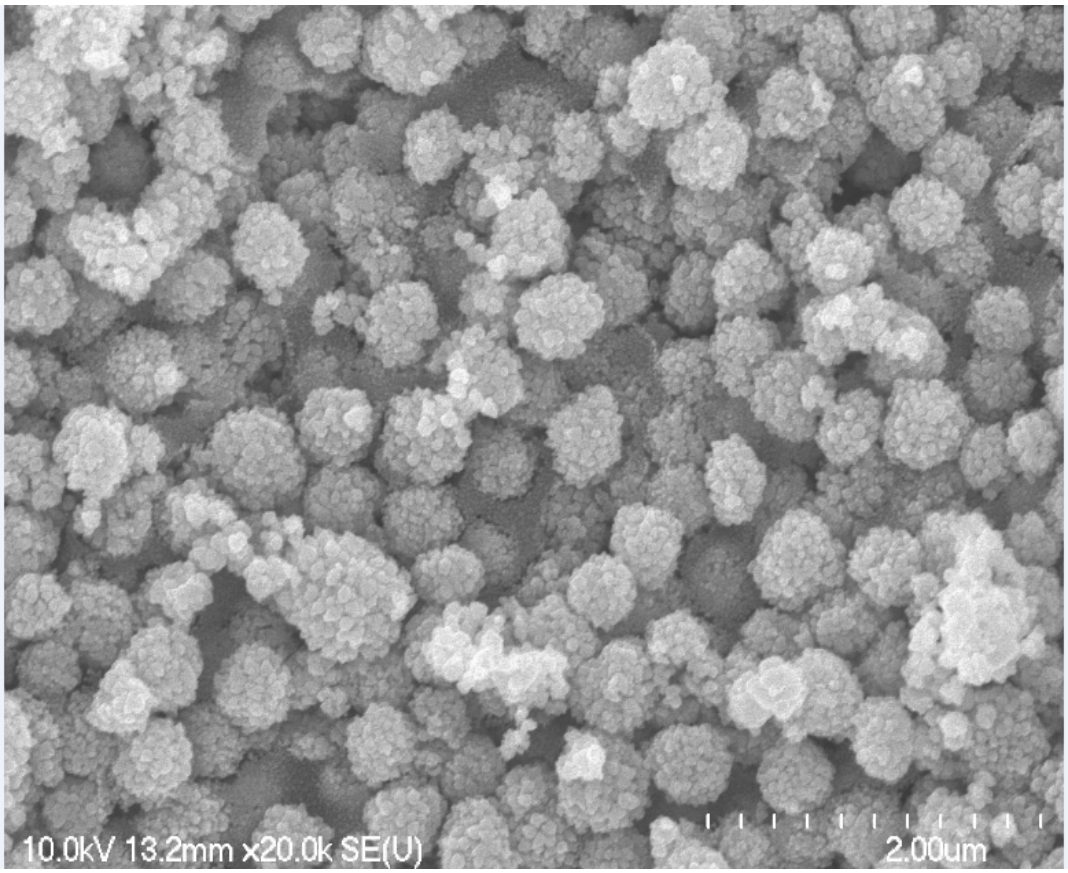

Figure 4.6: Flower shape of Scanning Electron Microscope images for S-2ZnO NPs.

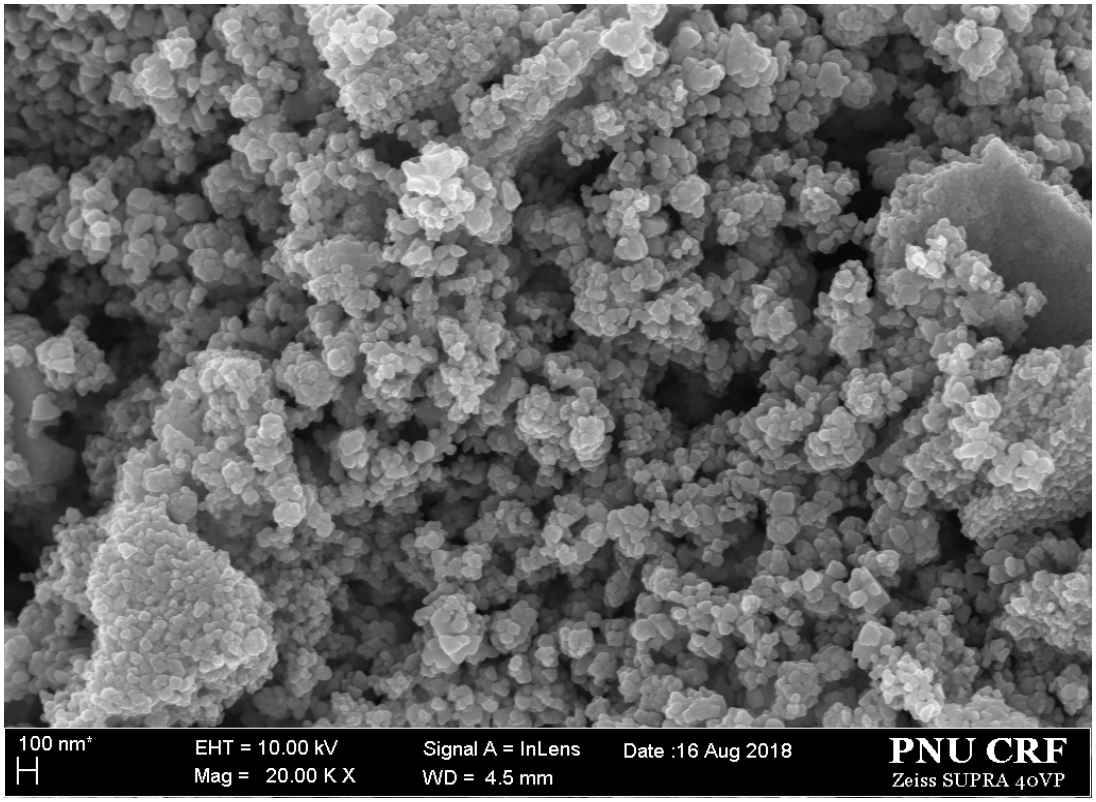

Fig.4.7. The spherical shape image of Scanning electron microscope for S-4 ZnO NPs

4.3. UV-Vis absorption Analysis

Fig. 4.7. below shows the UV–Visible absorption spectra of S-1, S-3, S-4, S-5 and S-6 ZnO NPs which exhibits a clear absorbance peak at 380 nm, 383 nm, 383 nm, 384 nm, and 385 nm respectively. Due to their nanodimension all the synthesised ZnO NPs exhibit blue shifted absorbance peak as compared to their bulk counterpart having absorbance peak at 386 nm at room temperature [38– 40].

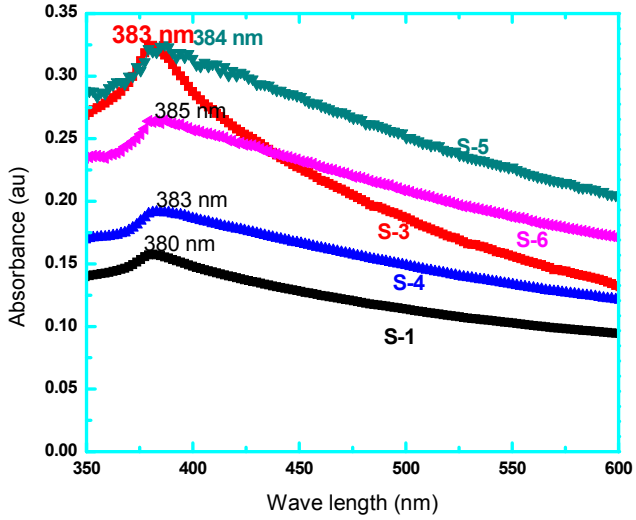

Fig 4.8: Absorption spectra of S-1, S-3, S-4, S-5 and S-6 ZnO NPs.

4.8. Emission Spectra analysis

Fig.4.7. Shows the emission spectra of ZnO NPs excited at wavelength of 325nm and emission recoded between 350 -700nm for each sample. Generally, the emission spectra of ZnO NPs consist of two emission bands: one in the UV-region near 370-400 nm and a broad band in the visible regions 400- 700 nm. Our samples exhibit UV emission peak at 398 nm, 391 nm, 398 nm, 386 nm and 382 nm for S-1, S-3, S-4, S-5, S-6 respectively. This is due to the recombination between the electrons in the conduction band and holes in the valance band. The broad violet region visible emission peaks at 412 nm and 429 nm for S-1 and S-3 The other blue-green emission peaks at 474 nm for S-5 and S-6 The violet emission peak at 417 nm is ascribed to an electron transition from a shallow donor level of neutral Zn_i to the top level of valance band [45,46]. The blue emission centered on 450 nm is attributed to singly ionized V_{Zn}^{-}. A blue green emission centred at 481 nm is due to radiative transition of electron from the shallow donor level

of Zn_i to an acceptor level of neutral V_{zn} [47]. The green emissionin our sample S-3, S-4, S-5, S-6was observed at 522nm, 518nm, 523nm, 519nm respectively due to radiative transition from conduction band to the edge of the acceptor level of O_{Zn} caused by oxygen antisites (O_{Zn}) [47]. The peak emission of the samples is independent of the temperature butemission intensity is temperature dependent i.e it increases as the temperatures of the samples increased.

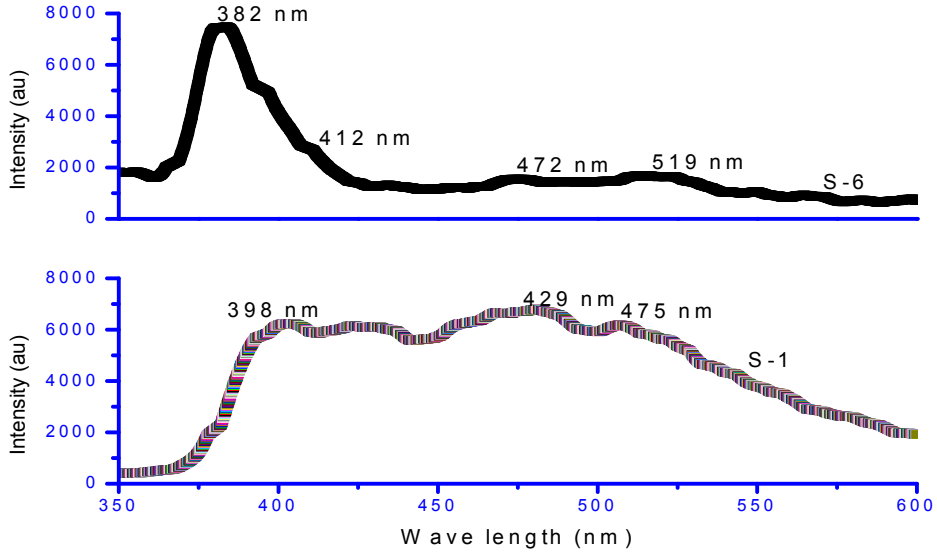

Fig. 4.9. The emission spectra of S-1 and S-6 ZnO NPs

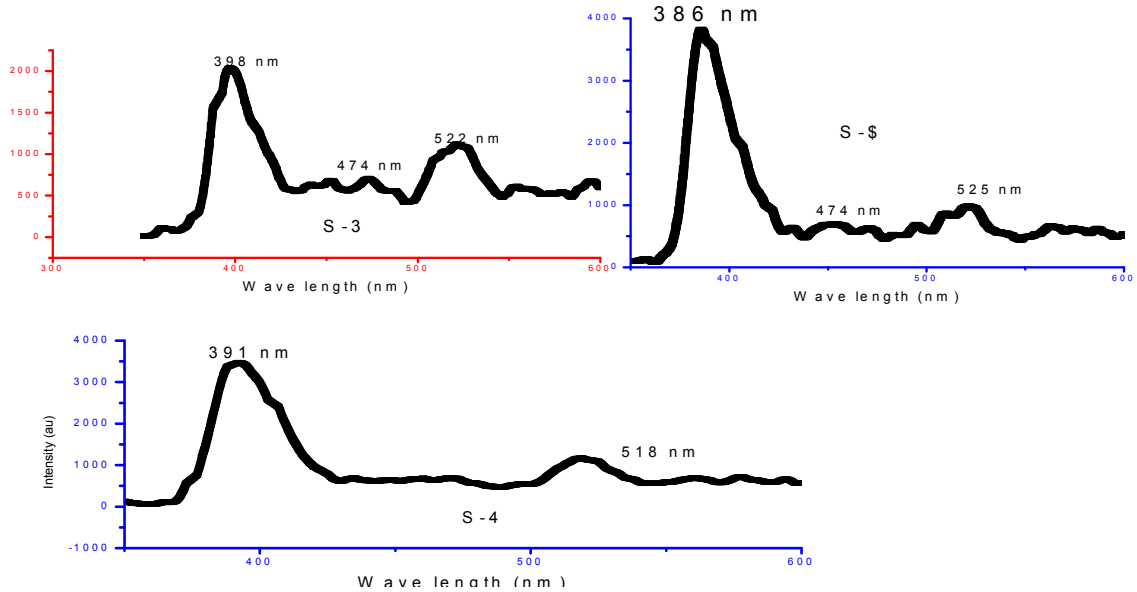

Fig. 4.10. The emission spectra of S-3, S-4 and S-5ZnONps.

4.4. Antimicrobial activity of the ZnO nanoparticles

Table4.4: show the MIC of S-1, S-3, S-4 and S-5 ZnO NPs for each microbials the most MIC to inhibate was belongs to S-3 ZnO NPs which shows it is excellent antimicrobials

Fig4.11 shows the presence of an inhibition zone clearly indicated the antibacterial effect of ZnO nanoparticles. Fig4.10a, b shows inhibition zone increase as concentration increase this result was compared with the result of gentamicin. Zone of inhibition due gentamicin was equal to zone of inhibition of 12.63mM S-1 ZnO NPs. Zone of inhibition due gentamicin was 21% lower than 12.63mM of S-3 ZnO NPs for S. aureus. But zone of inhibition due to gentamicin is 13% greater than 12.63mM of S-4 ZnO NPs for S. aureus. In general, all synthesized ZnO nanoparticles were showed admirable antimicrobial activity and it is comparable with gentamicin inhiation zone.

Fig4.10a, b Gram-negative bacteria *E. coli* and *P. aeruginosa* had inhibition zone sizes that were 6.66%,17.24% and 14.28% lower than Gram-positive bacteria *S. aureus B. subtilis and S. typhi*

in the case of S-1 ZnO NPs. In the case of S-2 ZnO NPs Gram-negative bacteria *E. coli* and *P. aeruginosa* had zone inhibition sizes that were 21%, 11.76% and 9% lower than Gram-positive S. aureus, *B. subtilis* and *S. typhi* bacteria. This observation could also be indicative of higher Gram-negative resistance against ZnO NPs over Gram-positive bacteria. Our finding in agreement with [49] who reported that the ZnO nanoparticle effect is more pronounced against Gram-positive bacteria than Gram-negative bacteria.

Table4.4.the measured value of MIC for S-1, S-3, S-4 and S-5 ZnO NPs on pathogenic bacteria and fungus using well diffision method

Name of pathogenic bacteria and fungus	MIC(mM)			
	S-1	S-3	S-4	S-5
E. coli	0.3660±0.15	0.23±0.15	0.6±0.2	0.4±0.2
P. auruginosa	0.6±0.23	0.35±0.23	0.86±0.11	0.93±0.23
B. subtillis	0.33±0.11	0.46±0.3	1±0.2	1.3±0.6
S. aurues	0.4±0.2	0.33±0.23	1.13±0.41	1.4±1.15
S. typhi	0.66±0.11	0.6±0.2	1±0.24	1.23±0.15
C. albicans	1±0	1.06±0.11	1.46±0.11	1.46±0.11

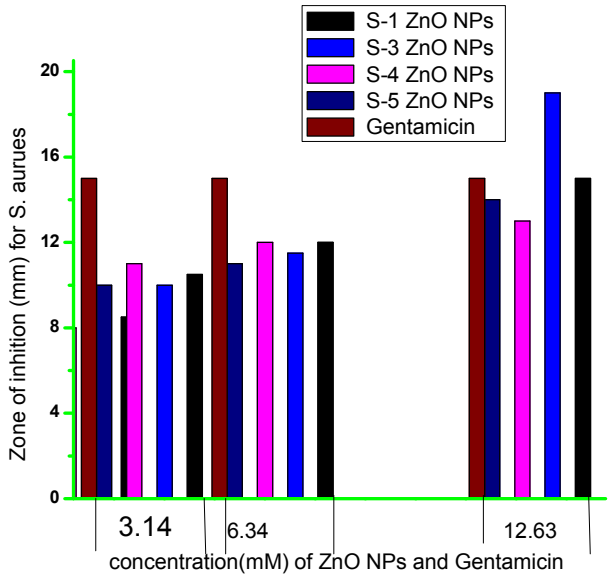

Fig4. 11Thebar graphs showing zone of inhibition introduced by S-1, S-3, S-4, S-5 ZnO NPs at 3.14mM, 6.34mM, 12.63mM and Gentamicinagainst S. aureus

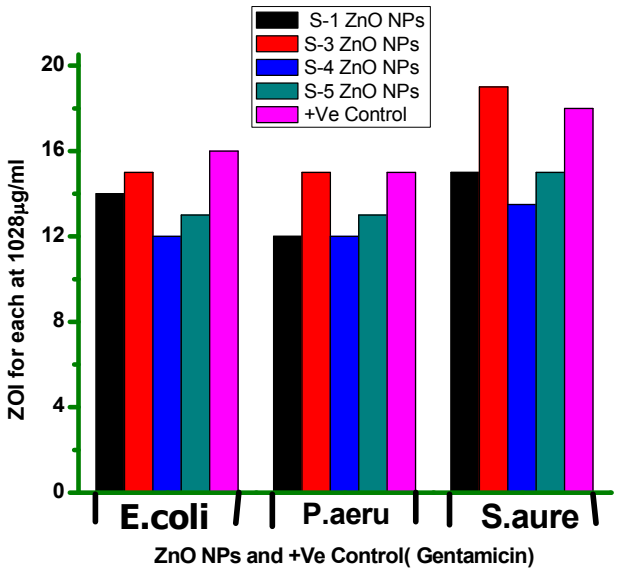

a

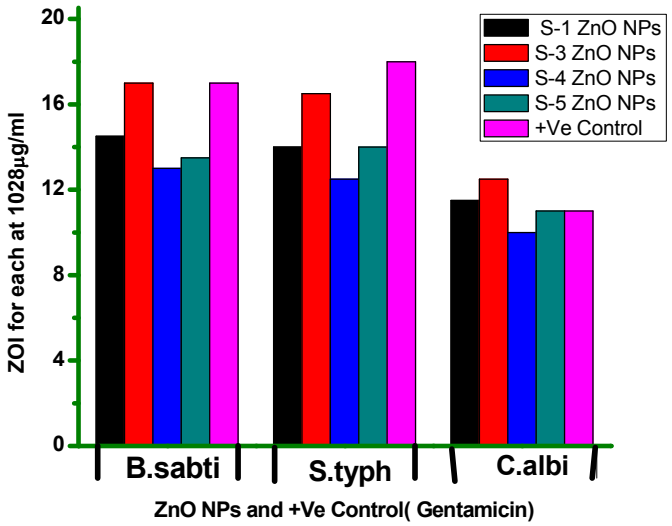

b

Fig 4.113a,b thebar graphs showing zone of inhibition introduced by S-1, S-3, S-4, S-5 ZnO NPs and Gentamicinagainst E. coli, P. aeruginosa, S. aureus, B. subtills, S. typhi and C. albicans

a

b

Fig4.13 a,b shows inhibition zone of S-3nO ZnO NPs on E.coli and S-1 ZnO NPs on S. aureus

5 Conclusions and Recommendations

5.1 Conclusions

Zinc oxide NPs have been synthesised from precursor like zinc acetate dihydrate and zinc nitrate hexahydrate using Sol-gel,thermal decomposition and Precipitation method respectively. The synthesised ZnO NPs were characterized by using spectroscopy technique such as X-ray diffraction (XRD), Scanning Electron Microscopy (SEM), UV-Vis Spectroscopy, Fluorescence Spectroscopy and FTIR Spectroscopy. The averaged crystallite size of the synthesisedZnO NPs was 22.04 ± 2 nm, 29.38 ± 2 nm, 29.92 ± 1 nm, 29.30 ± 4 nm, 36.90 ± 3 nm, 41.67 ± 2 nm for S-1, S-2, S-3, S-4, S-5 and S-6 synthesized ZnO NPs respectively and. and SEM image of S-2 and S-4 ZnO NPs indicate the increment in the particle size of ZnO NPs as synthesis methed is changed.There was variation in UV-Vis absorption peaks of synthesized ZnO NPs and energy band gap of synthesized ZnO NPs was 3.48 eV, 3.43eV, 3.43 eV, 3.43 eV, 3.41eV and 3.40 eV for S-1, S-3, S-4, S-5 and S-6 respectively which indicates that the optical property of ZnO NPs influenced by size. The ZnO nanoparticles were showed two emission bands, an ultraviolet (UV) emission band due to the electronic transition from conduction band edge to valence band, and visible emission band due to defects that are related to deep level emissions. The S-1, S-3, S-4 and S-5 ZnO NPs were applied for antimicrobial applications. S-3 ZnO NPs was excellent antimicrobial ZnO NPs Generally, the result in this study indicates that ZnO nanoparticles are moreeffective against Gram-positive bacteriacompared to Gram-negative bacteria.

References

[1] Sahoo, S. (2010): Socio-ethical issues and nanotechnology development: perspectives

from India. IEEE Conference on Nanotechnology (IEEE-NANO), 1205–1210.

[2] Yadav, V. (2013): Nanotechnology, big things from a tiny world: areview. AEEE, 3(6): 771–778.

[3] Tomar, R.S., Shrivastava, V. and Chauhan, P.S. (2015): Nanobiotechnology: A potential tool for biomedics. World Journal of Pharmacy and Pharmaceutical Sciences, 4 (5): 1929-1943.

[4] Murty, B.S., Shankar, P., Raj, B., Rath, B.B. and Murday, J. (2013): Text book of nanoscience and nanotechnology, Berlin, Germany.

[5] Wyckoff, R.W.G. (1964): Crystal Structures, 2nd ed; Wiley: New York.

[6] Rai, M., Yadav, A. and Gade, A. (2009): Silver nanoparticles as a new generation of antimicrobials. Biotechnology Advances, 27(1): 76–83.

[7] Awodugba, A.O. and Ilyas, A.M.O. (2013): Synthesis and characterization of ZnO nanoparticles with zinc chloride as zinc source. Asian Journal of Natural and Applied Sciences, 2(2):41- 44.

[8] Ellmer, E. K., Klein, A. and Rech, B. (2008): Transparent conductive zinc oxide. Springer, Berlin, Germany.

[9] Anderson, J. and Chris, G.V.W. (2009): Fundamentals of zinc oxide as a semiconductor. Reports on Progress in Physics, 72: 1-29.

[10] Jayanta, K. B. (2012): Synthesis and characterization of ZnO nanoparticles. A thesis, National Institute of Technology, Rourkela, India.

[11] Segets, D., Gradl, J., Taylor, R.K., Vassilev, V. and Peukert, W. (2009): Analysis of optical absorbance spectra for the determination of ZnO nanoparticle size distribution, solubility, and surface energy. ACS Nano, 3(7): 1703–1710.

[12] Ling-min, Y., Xin-hui, F., lei, C., Jing-yi, S. and Wen, Y. (2012): Shape-controlled cluster growth of ZnO nanoflowers using sol–gel method. Micro and Nano Letters, 7: 1046-1048.

[13] Darroudia, M., Sabouric, Z., Oskueeb, R.K., Zake, A.K., Kargarc, H. and Hamid, M.H.N.A. (2013): Sol–gel synthesis, characterization and neuro toxicity effect of zinc oxide nanoparticles using gum tragacanth. Ceramics International, 24: 345-349.

[14] Singh, D.K., Pandey, D.K., Yadav, R.R. and Singh, D. (2012): A Study of nanosized zinc oxide and its nanofluid. Pramana Journal of Physics, 78(5):759-766.

[15] George, K.C., Soosen, S.M. and Lekshmi, B. (2009): Optical properties of ZnO nanoparticles. SB Academic Review, 16(1-2): 57-65.

[16] Gunasekaran, S., Shi, L. and Zhou, J. (2008): Low temperature fabrication of ZnO-whey protein isolate nanocomposite. Materials Letters, 62(28): 4383–4385.

[17] Jalal, R., Abareshi, M., Goharshadi, E.K., Moosavi, M., Yousefi, A. and Nancarrow, P. (2010): ZnO nanofluids: green synthesis, characterization and antibacterial activity. Materials Chemistry and Physics, 121(1–2): 198–201.

[18] Premanathan, M., Karthikeyan, K., Jeyasubramanian, K.andManivannan, G. (2011): Selective toxicity of ZnO nanoparticles toward Gram-positive bacteria and cancer cells by apoptosis through lipid peroxidation. Nanomedicine: Nanotechnology, Biology and Medicine, 7(2): 184–192.

[19] Basha, S.K., Lakshmi, K.V. and Kumari, V.S. (2016): Ammonia sensor and antibacterial activities of green zinc oxide nanoparticles. Sensing and Bio-Sensing Research 10: 34-40.

[20] Qu, F. and Morais, P.C. (2001): The pH dependence of the surface charge density in oxide-based semiconductor nanoparticles immersed in aqueous solution. IEEE Transactions on Magnetic, 37: 2654–2656.

[21] Jagadish, C. and Pearton, S. (2012): Basic properties and applications of ZnO. The Australian national University, Canberra, ACT 0200, Australia.

[22] Kolodzimejczak, A. and Jesionowwski T. (2014): "Zinc Oxide from synthesis to application and reviewmaterials," Journal of microbial methods, 7(4) : 2833.

[23] Surya, P. G. (2012): Synthesis and characterization of zinc oxide nanoparticles by sol-gel methods. A thesis, National Institute of Technology, Rourkela, India.

[24] Paula, E., Jane, R.C., Renato, S.C. and Eber, A.A.M. (2012): Zinc oxide nanoparticles:Synthesis, antimicrobial activity and food packaging applications. Food and BioprocessTechnology, 5:1447–1464.

[25] Cullity, B.D., Stock, S.R. (2001): Elements of X-ray diffraction, 3rd edn. Prentice Hall, New Jersey

[26] Saleem, M., Fang, L., Ruan, H.B., Wu, F., Huang, Q.L., Xu, C.L., Kong, C.Y. (2012): Effect of zinc acetate concentration on the structural and optical properties of ZnO thin films deposited by sol-gel method. Intl. J. Phy. Sci. 7(23), 2971–2979.

[27] Seetawan. U., Jugsujinda, S., Seetawan, T., Ratchasin, A., Eu-vananont, C., Junin, C.,

[28] Thanachayanont, C.,Chainaronk, P. (2011): Effect of calcinations temperature on crystallography and nano-particles in ZnO disk. Maters. Sci. Appls. 2, 1302–1306.

[29] Seetawan, U., Jugsujinda, S., Seetawan, T., Ratchasin, A., Eu-vananont, C., Junin, C., Thanachayanont, C., Chainaronk, P. (2011): Effect of calcinations temperature on crystallography and nano-particles in ZnO disk. Maters. Sci. Appls. 2, 1302–1306

[30] Ahmed, M., Abd, E., Sarhan, A., and Hasan, A., (2016): "Preparation and characterization of ZnO NPs by simple precipitation methods," Journal lumin, 4 (3),65.

[31] Spanhel, L. (2006): Colloidal ZnO nanostructures and functional coatings. A survey. J Sol-Gel Sci Techn. 39, 7-4.

[32] Sibilia, P. (1998): A guide to materials characterization and chemical analysis.VCH, New York. Suhandro, P.P. and Rosari, S. (2012): Synthesis and spectroscopic characterization of undoped nanocrystalline ZnO nanoparticles prepared by co-precipitation. Journal of Material Science and Applications, 3: 530-537.

[33] West, A.R. (2003): Solid state chemistry and its applications. John Wiley &Sons, Singapore, Indian.

[34] Kommu, N. (2014): Applications of fluorescence spectroscopy. International Journal of Chemical and Pharmaceutical Sciences, 5: 18-21.

[35]Sawai, J., Shoji, S., Igarash, H., Hashimoto, A., Kokugan, T., Shimizu, M. and Kojima, H.

(1998): Hydrogen peroxide as an antibacterial factor in zinc oxide powder slurry. Journal of Fermentation and Bioengineering, 86(5): 521–522.

[36] Zhang, L., Ding, Y., Povey, M. and York, D. (2008): ZnO nanofluids—a potential antibacterial agent. Progress in Natural Science, 18(8): 939–944

[37]Talebian, N., Amininezhad,S.M, M. Doudi, M. (2013): Controllable syn-thesis of ZnO nanoparticles and their morphology-dependent antibacterial and optical properties. J. Photochem. Photobiol. 120, 66–73.

[38]Ma, J., Liu, J. Y. Bao,y,. (2013): Zhang, Synthesis of large-scale uniform mulberry-like ZnO particles with microwave hy-drothermal method and its antibacterial property. Ceram. Int. 39(3), 2803–2810.

[39] Zhang, L., Jiang, Y., Ding, M., (2007): Investigation into the antibacterial behaviour of suspensions of ZnO nanoparticles (ZnO nanofluids). J. Nanopart. Res. 9(3), 479–489.

[40] Zhang, J., (2011): Silver-coated zinc oxide nanoantibacterial synthesis and antibacterial activity characterization, International Conference on Electronics and Optoelectronics (ICEOE), 3, 94-98.

[41] Nirmala, M., Rekha, K., Anukaliani, A., Samdarshi, S., (2010): Photocatalytic activity of ZnOnanopowders synthesized by DC thermal plasma. Afr. J. Basic Appl. Sci. 2(5–6), 161–166. 66.

[42] Bao, I.S.J., Su, Z., Gurwitz, R., Capasso, F., Wang, X.,Ren, Z., (2011): Photoinduced oxygen release and persistent photoconductivity in ZnO nanowires. Nanoscale Res. Lett. 6(404),

1-7.

[43] Baruah, S., Mahmood, M.A., Myint, M.T.Z., Bora, T., Dutta, J., (2010): Enhanced visible light photocatalysis through fast crystallization of zinc oxide nanorods. Beilstein J. Nanotechnol. 1(1), 14–20.[49]

[44] Surti, A., Radha, S. and Garje, S.S. (2013): Study of the Antibacterial activity of ZnO nanoparticles. AIP Conf. Proc. 1512, 450.

[45] Mishra, S.K., Srivastava, S.K., Prakash, S.G., Yadav, R.S. (2010): Opto-Electron. Rev.18(2010)467

[46] Zhang, J., Sun, L.D., Yin, J.L., Su, H.L. C.H. Yan, (2002): Chem. Mater. 14 (2002) 4172.

[47] Singh D., Singh A., Mishr R., Tiwari S., and Srivastava O., (2011): "Synthesis, characterization and application of semiconducting oxide nanostructure," Bull, Mater. Scie. 31(319-325).

[48] Natsume, Y., Sakata, H., Hirayama, T., Yanagida, H., 72 (1992) 4203.

[49] Premanathan M, Karthikeyan K, Jeyasubramanian K, Manivannan G.:(2011) Selective toxicity of ZnO nanoparticles toward Gram-positive bacteria and cancer cells by apoptosis through lipid peroxidation. *Nanomedicine*. 7(184–192).